iScience, Volume ■ ■

Supplemental information

Selective aqueous anion recognition in an anionic host

Noa Bar Ziv, Chengwei Chen, Bryce da Camara, Ryan R. Julian, and Richard J. Hooley

Supplemental Information

Supplemental Figures

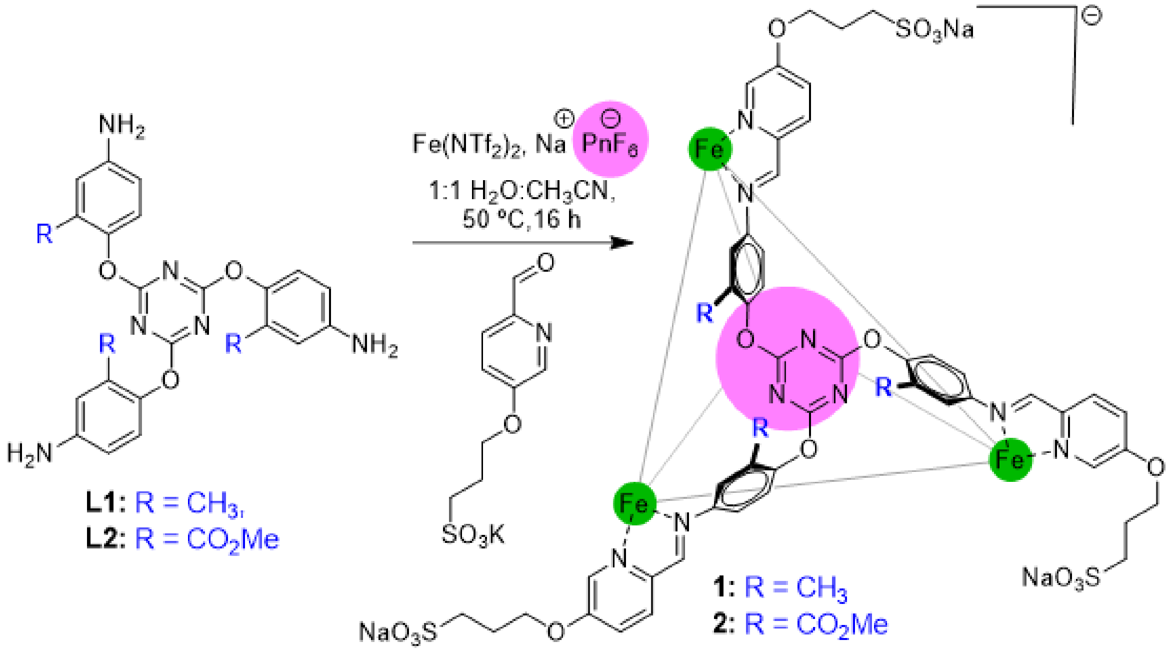

Figure S-1. Reaction scheme of self-assembled cages **1** and **2.** Related to Figure 1.

Cage Characterization

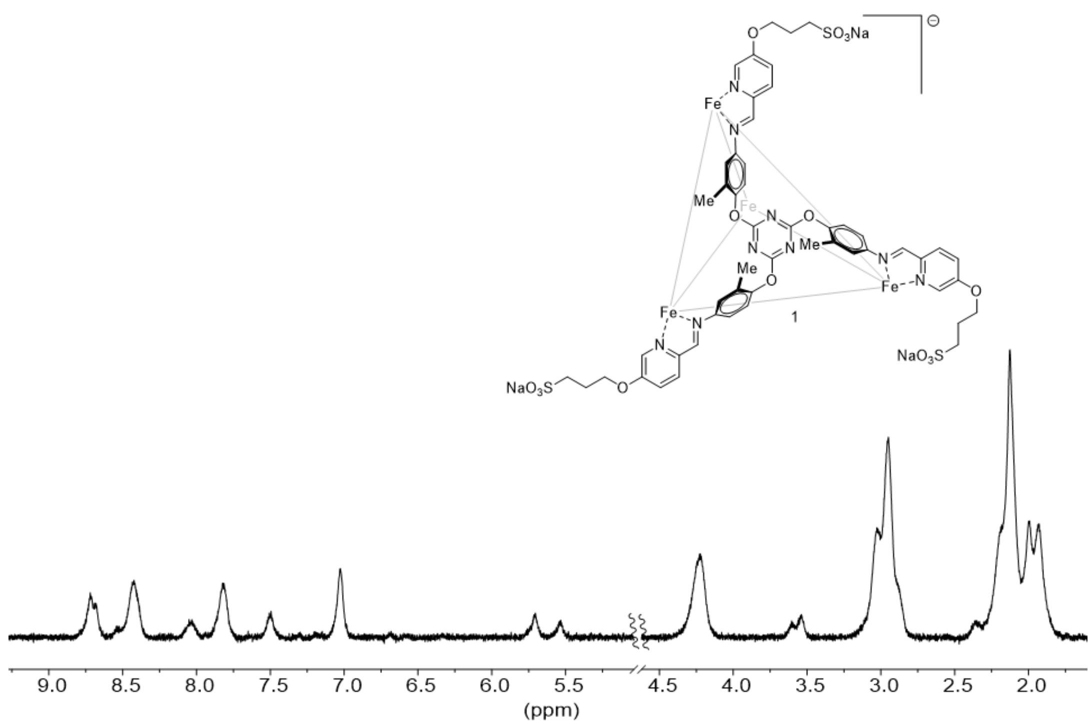

Figure S-2. [1]H NMR spectrum of cage **1** (D_2O, 400 MHz, 298K). Related to Figure 1 and STAR methods, synthesis of cage **1**.

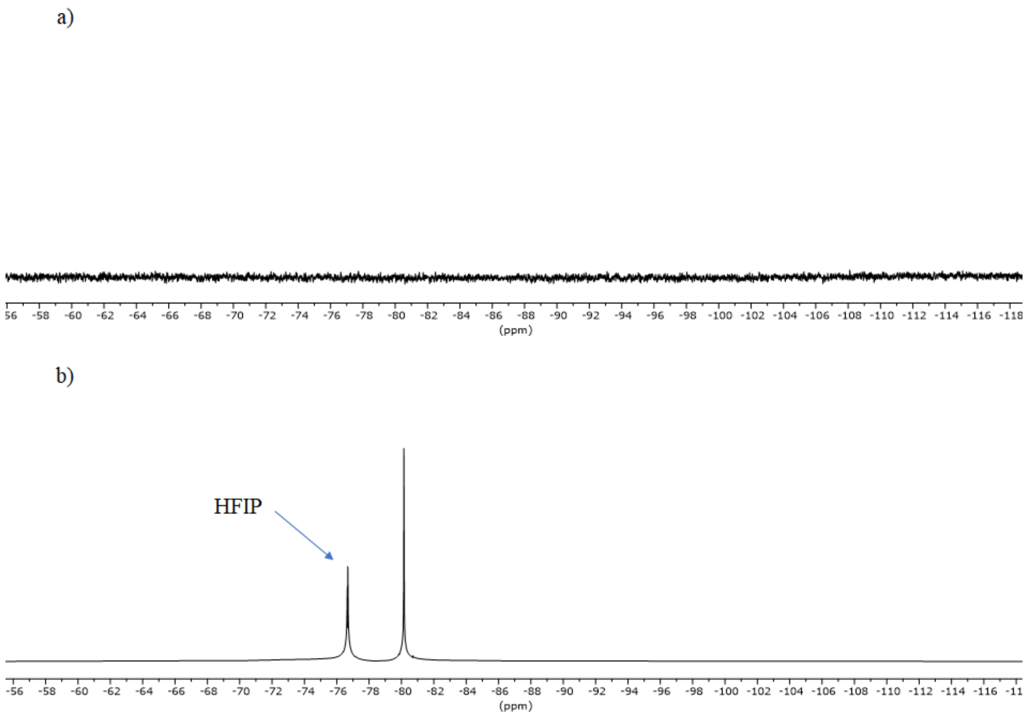

Figure S-3. ^{19}F NMR spectrum of a) cage **1** and b) $NaNTf_2$ with hexafluoroisopropanol (HFIP) as a standard (D_2O, 376 MHz, 298K). Related to Figure 1 and STAR methods, synthesis of cage **1**.

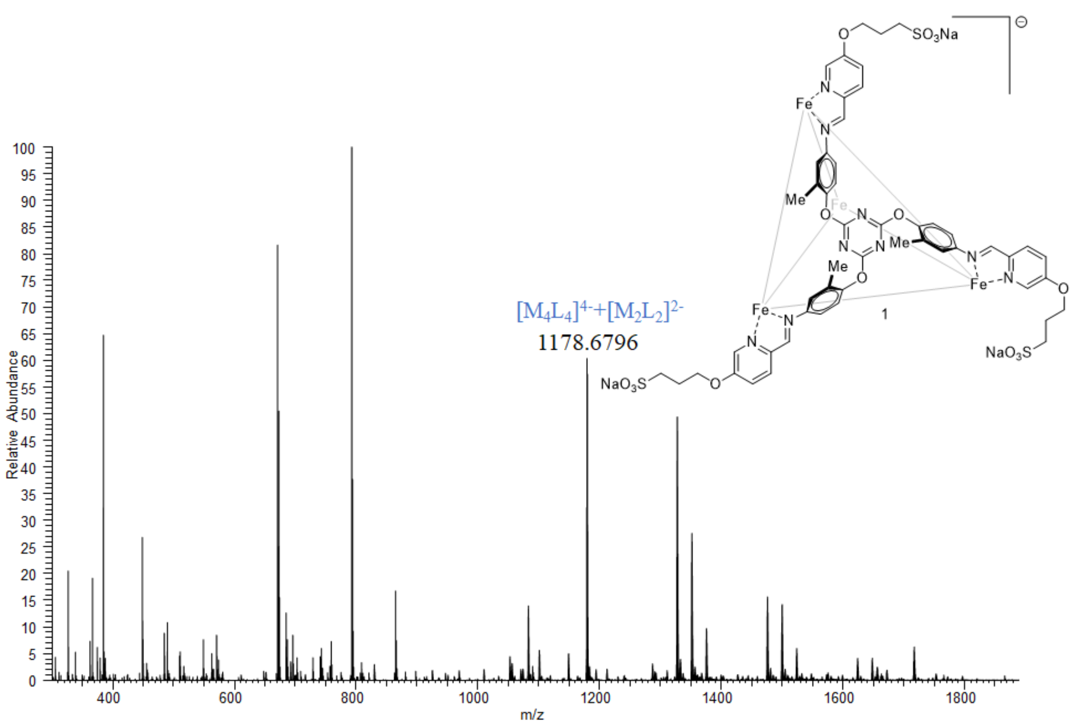

Figure S-4. ESI-MS spectrum of cage **1**. The flow rate, sheath gas flow rate, aux gas flow rate, spray voltage, capillary temperature, and the S-lens RF level were set to be 3 ul/min, 5 arb, 10 arb, 2.8 kV, 215 C, and 40% respectively. Full mass spectra were acquired with a resolution of r = 30,000. Related to Figure 1 and STAR methods, ESI-MS spectrum of cage **1**.

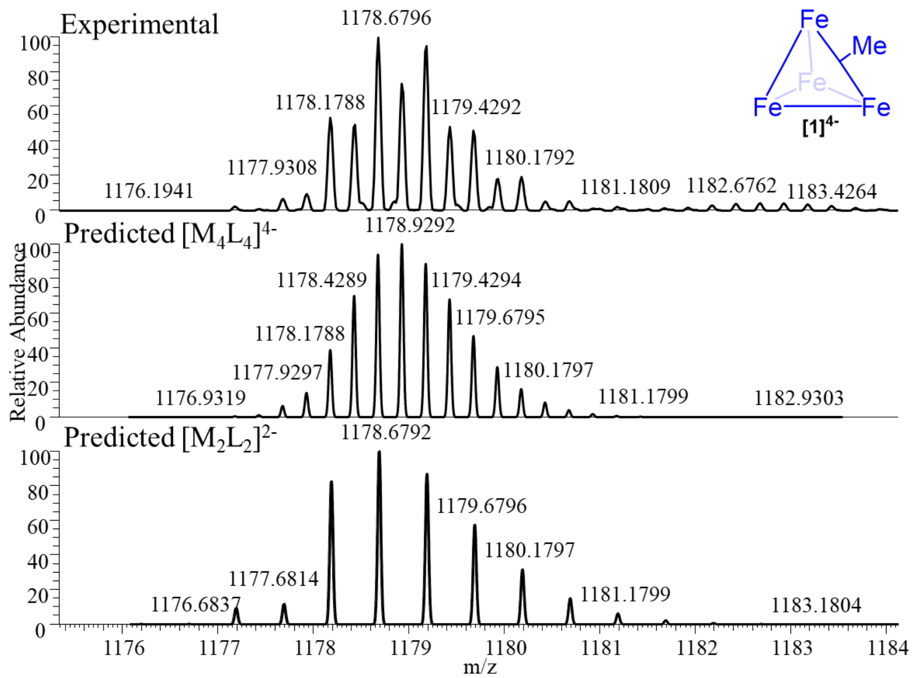

Figure S-5*.* Expansion of the ESI-MS spectrum of **1**, showing obtained and simulated isotope region [**1**]$^{4-}$ + $[Fe_2L_2]^{2-}$. Related to Figure 1 and STAR methods, ESI-MS spectrum of cage **1**.

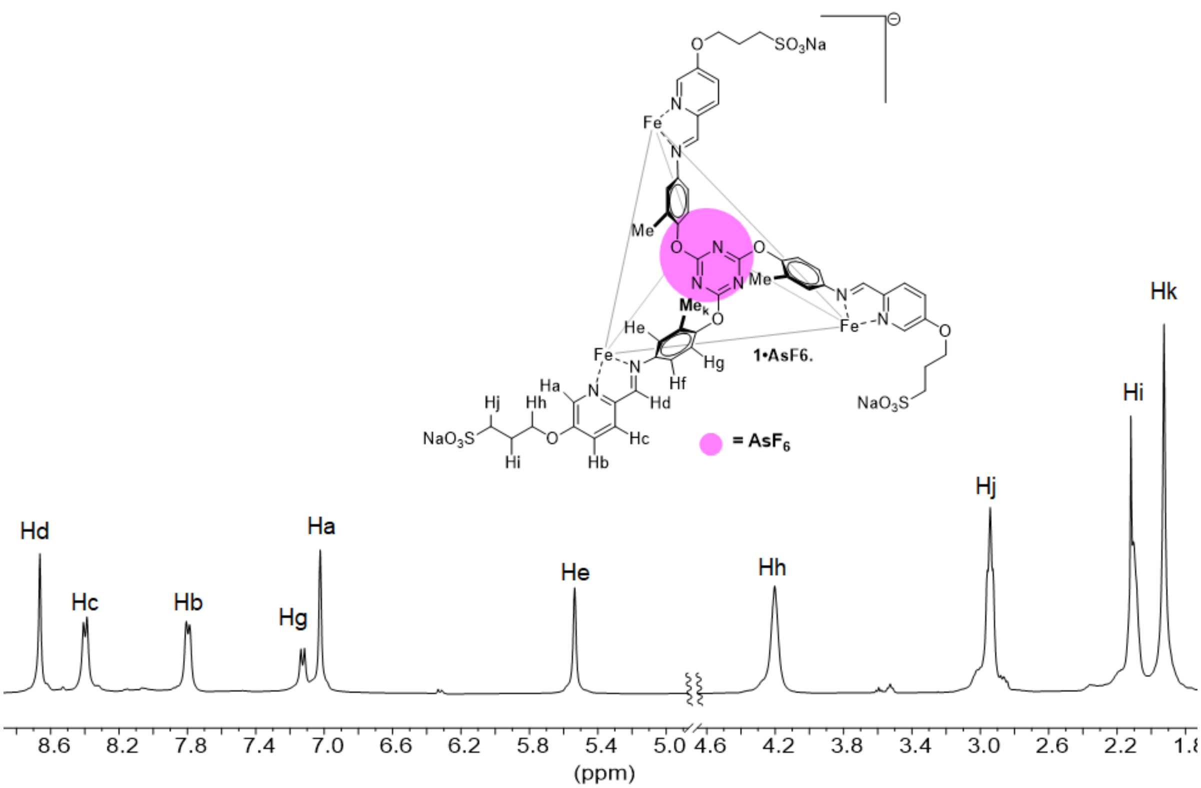

Figure S-6. ^{1}H NMR spectrum of cage **1•AsF$_6$.** The peak for H_f is under the HDO peak (D_2O, 400 MHz, 298K). Related to Figure 2 and STAR methods, synthesis of cage **1•AsF$_6$.**

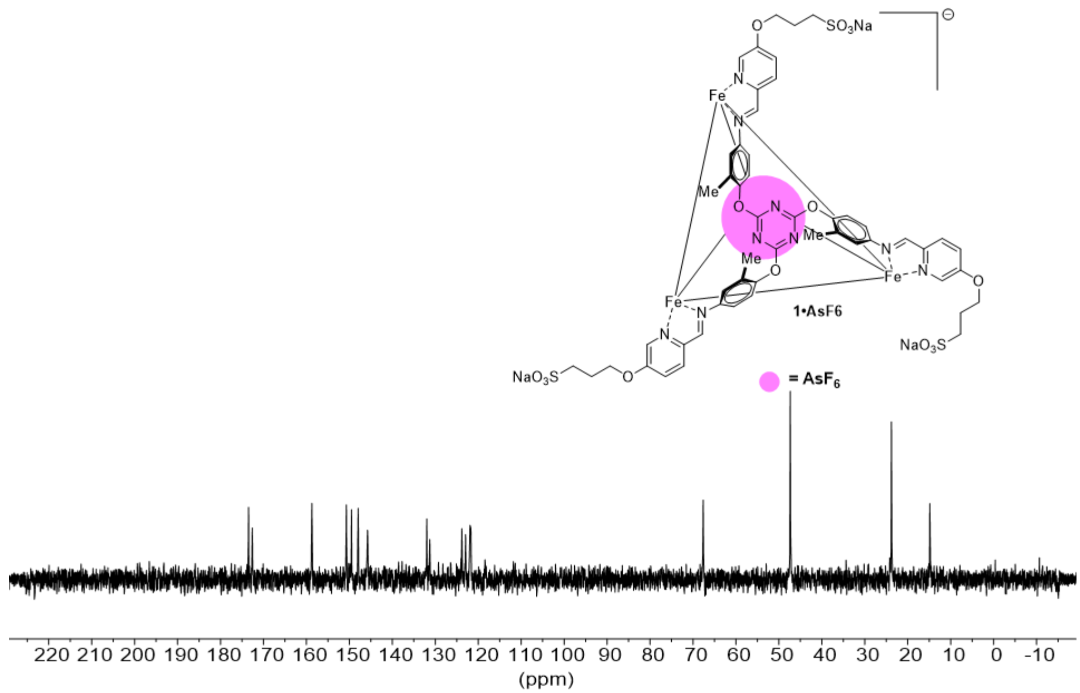

Figure S-7. $^{13}C\{^1H\}$ NMR spectrum of cage **1•AsF$_6$** (D_2O, 101 MHz, 298K). Related to Figure 2 and STAR methods, synthesis of cage **1•AsF$_6$.**

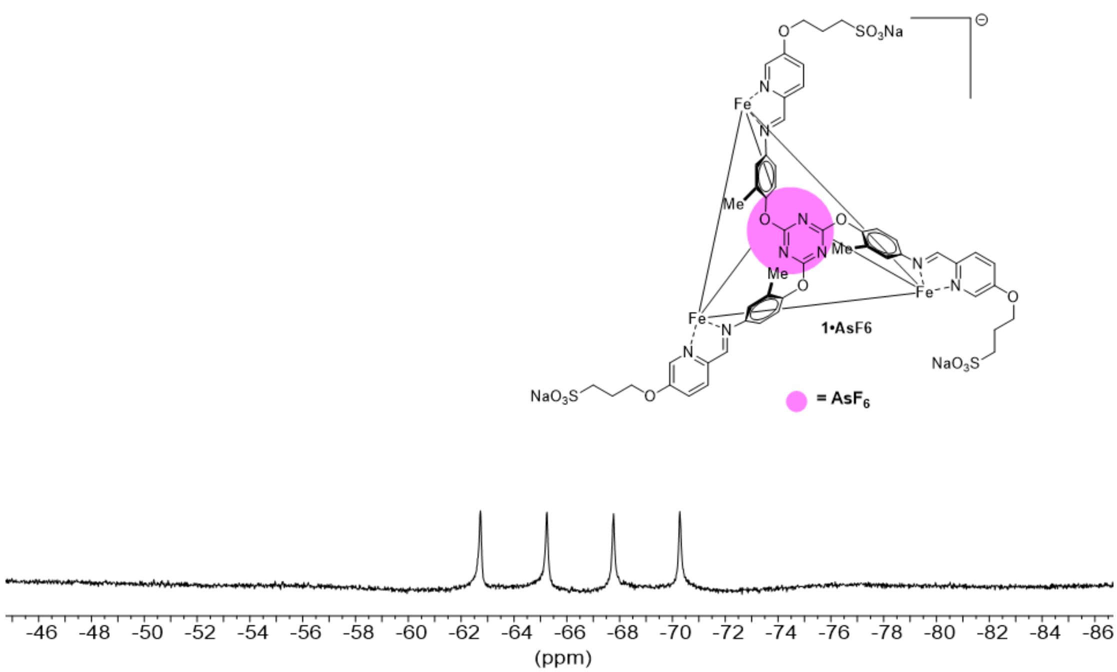

Figure S-8. ^{19}F NMR spectrum of cage **1•AsF$_6$** (D_2O, 376 MHz, 298K). Related to Figure 2 and STAR methods, synthesis of cage **1•AsF$_6$.**

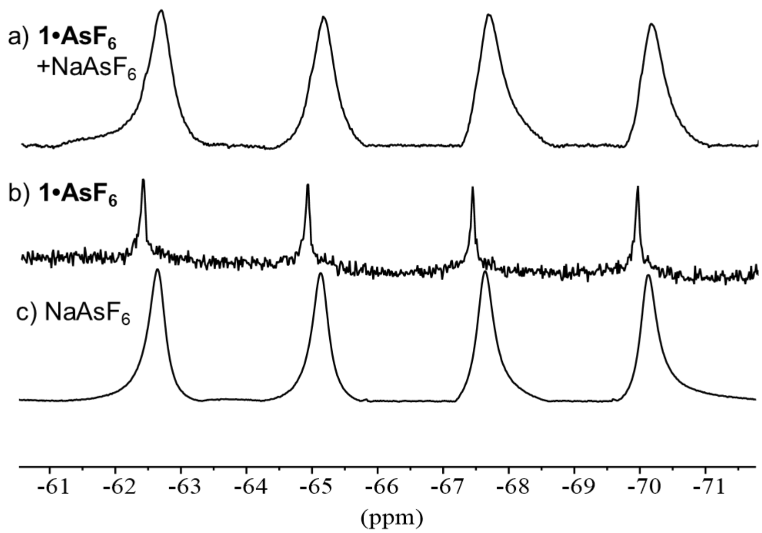

Figure S-9. [19]F NMR spectrum of a) **1•AsF$_6$** with added NaAsF$_6$; b) **1•AsF$_6$**; and c) NaAsF$_6$ (D_2O, 376 MHz, 298K). Related to Figure 2 and STAR methods, synthesis of cage **1•AsF$_6$.**

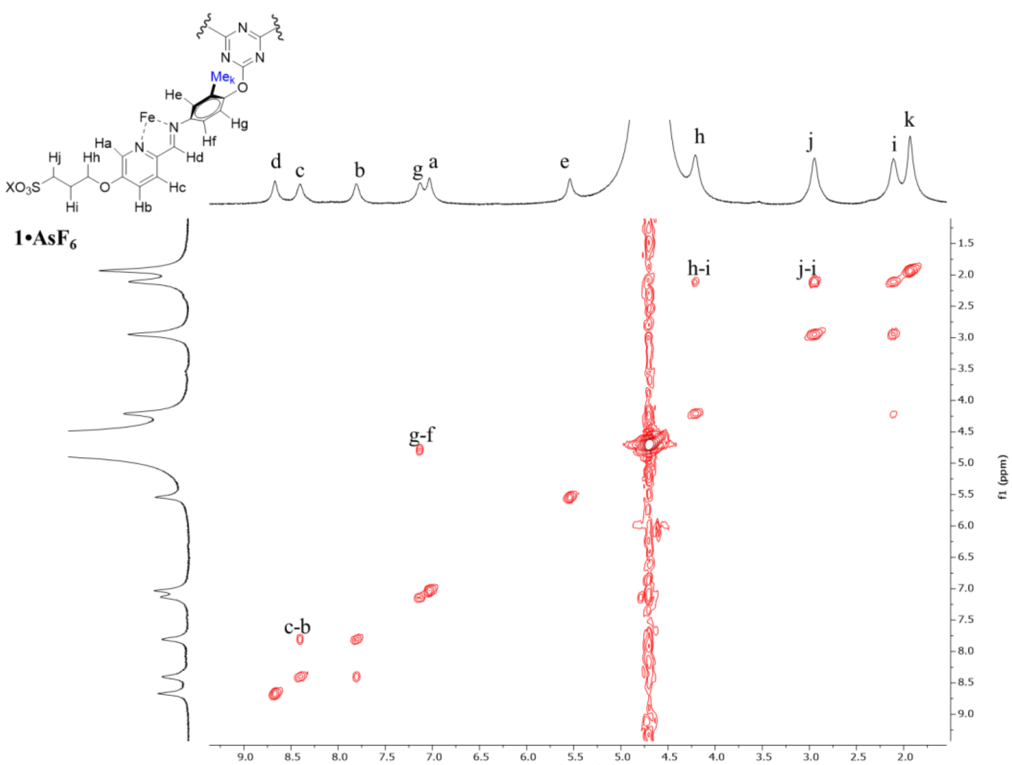

Figure S-10. gCOSY NMR spectrum of cage **1•AsF$_6$.** The peak for H_f is under the HDO peak (D_2O, 400 MHz, 298K). Related to Figure 2 and STAR methods, synthesis of cage **1•AsF$_6$.**

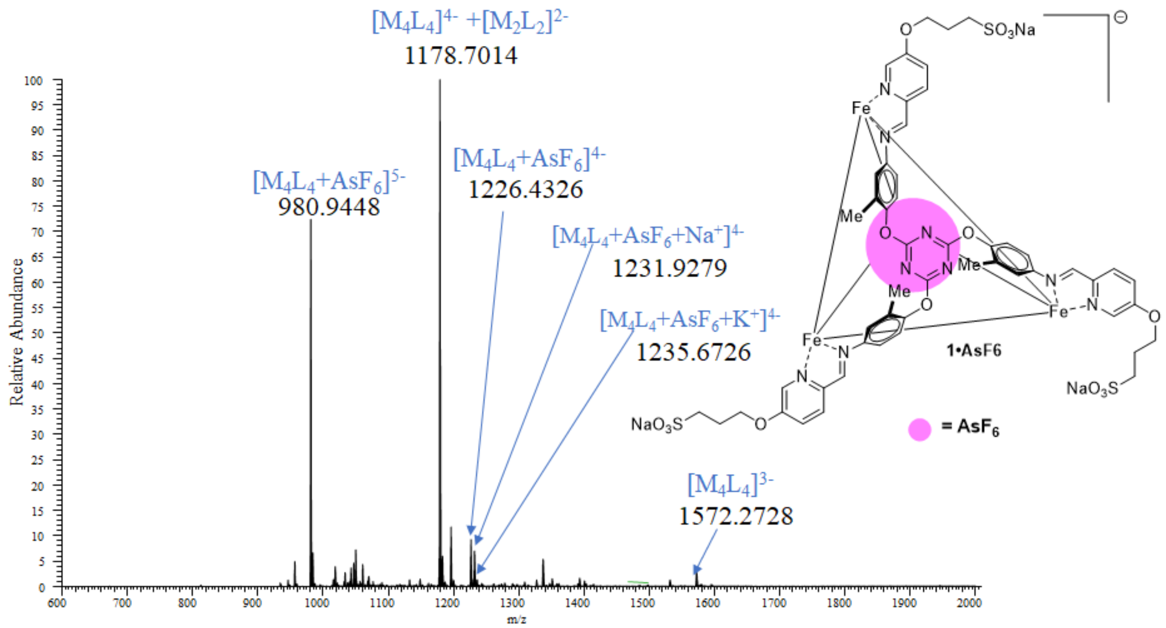

Figure S-11. ESI-MS spectrum of cage **1•AsF$_6$**. The flow rate, sheath gas flow rate, aux gas flow rate, spray voltage, capillary temperature, and the S-lens RF level were set to be 5 ul/min, 10 arb, 12 arb, 2.8 kV, 200 C, and 40% respectively. Full mass spectra were acquired with a resolution of r = 60,000. Related to Figure 2 and STAR methods, ESI-MS spectrum of cage **1•AsF$_6$**.

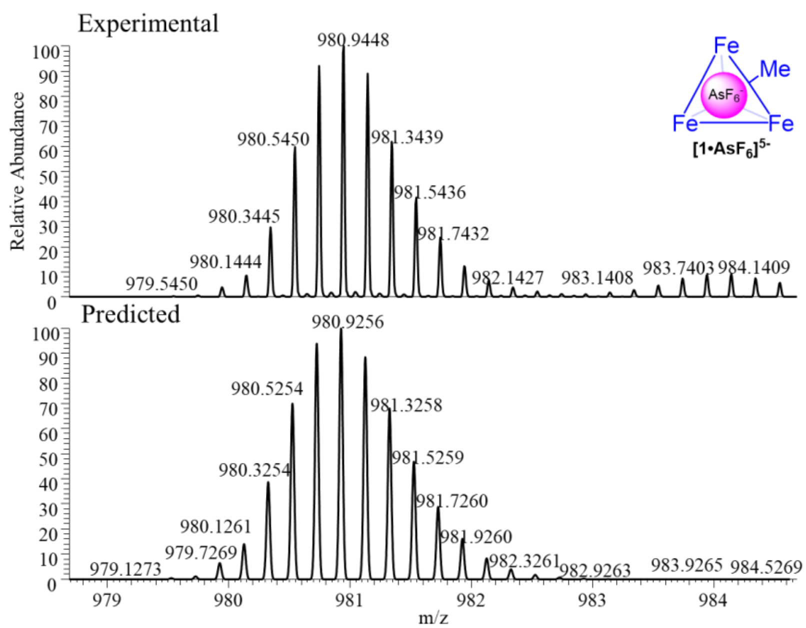

Figure S-12. Expansion of the ESI-MS spectrum of **1•AsF$_6$**, showing obtained and simulated isotope region [**1**•AsF$_6$]$^{5-}$. Related to Figure 2 and STAR methods, ESI-MS spectrum of cage **1•AsF$_6$**.

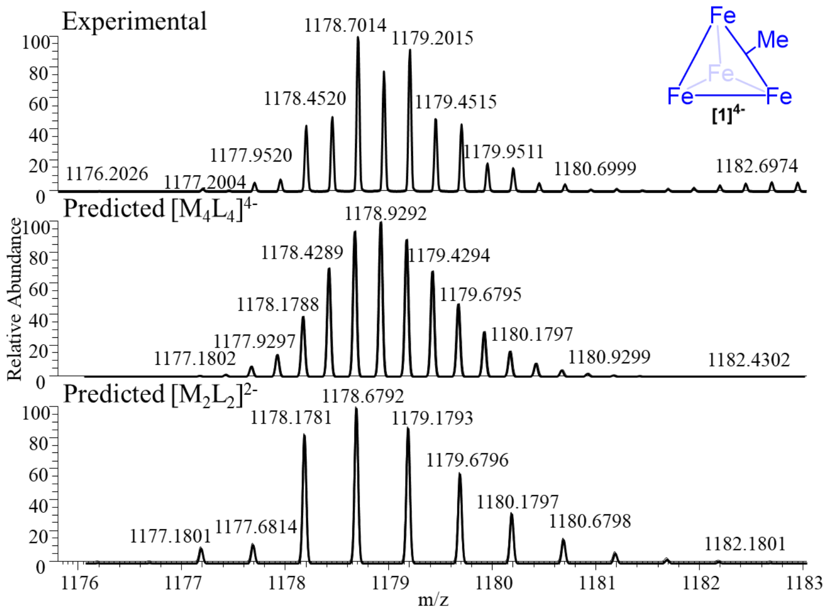

Figure S-13. Expansion of the ESI-MS spectrum of **1•AsF$_6$**, showing obtained and simulated isotope region [**1**]$^{4-}$ + [Fe_2L_2]$^{2-}$. Related to Figure 2 and STAR methods, ESI-MS spectrum of cage **1•AsF$_6$**.

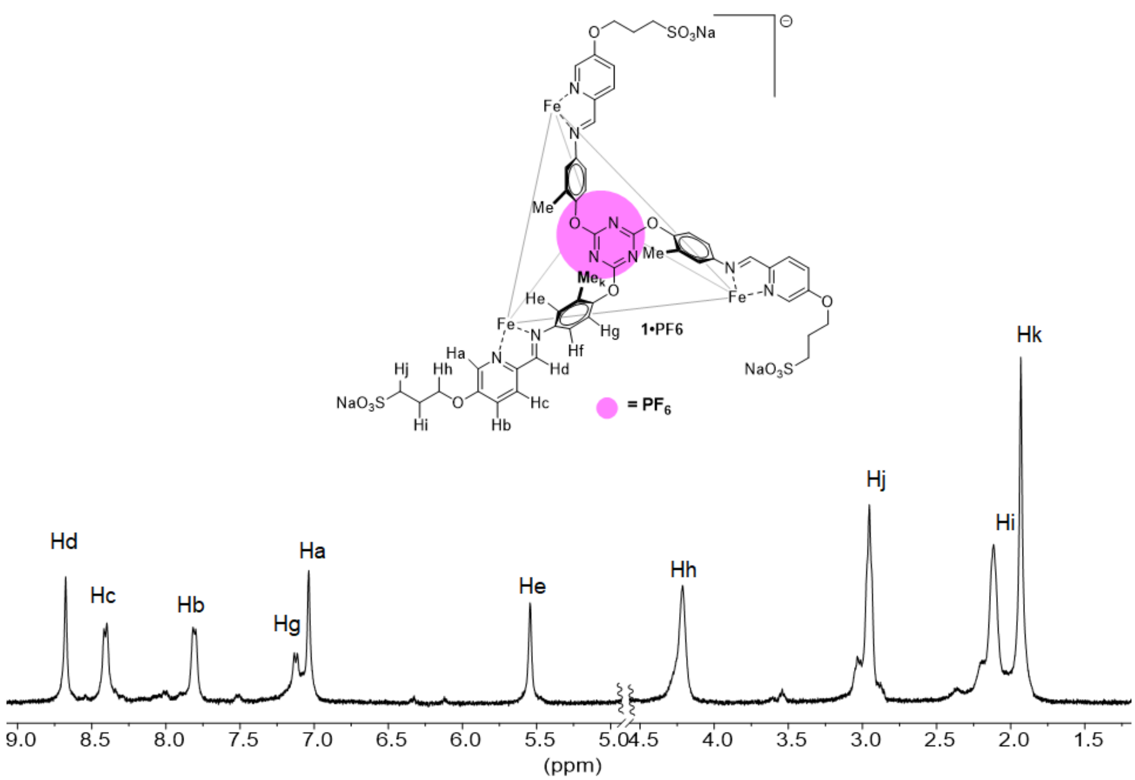

Figure S-14. ^1H NMR spectrum of cage **1•PF$_6$**. The peak for H_f is under the HDO peak (D_2O, 400 MHz, 298K). Related to Figure 1 and STAR methods, synthesis of cage **1•PF$_6$**.

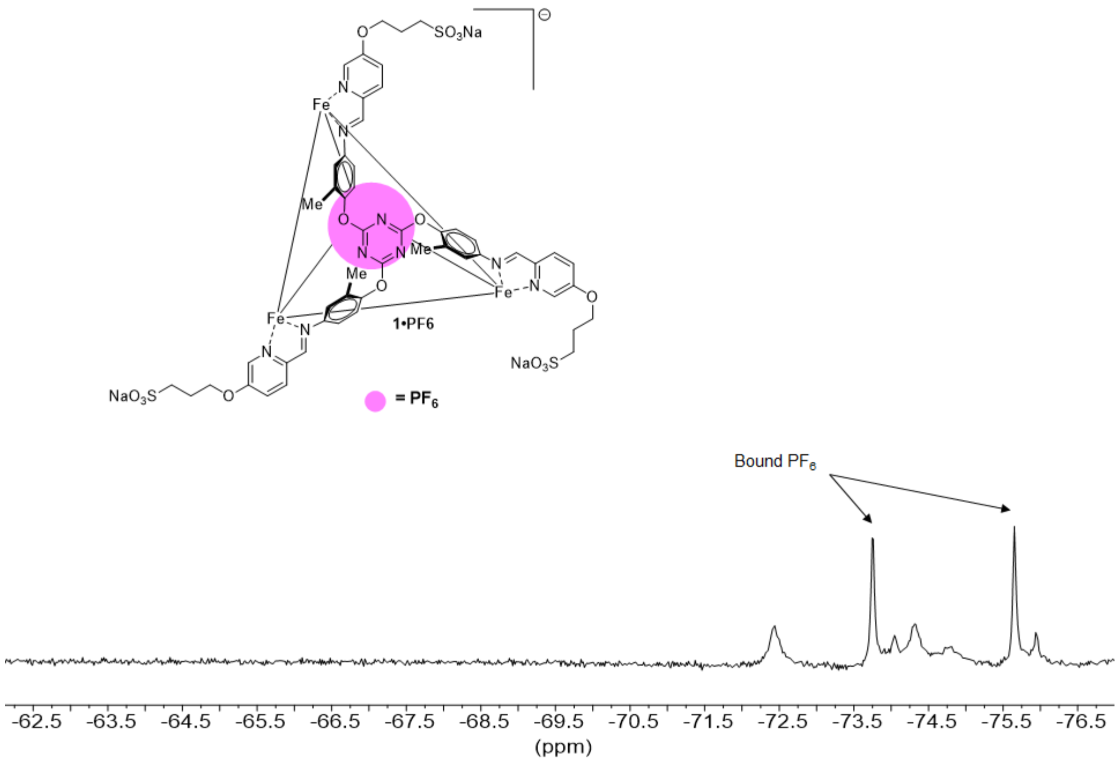

Figure S-15. ^{19}F NMR spectrum of cage **1•PF₆** (D_2O, 376 MHz, 298K). Related to Figure 1 and STAR methods, synthesis of cage **$1•PF_6$**.

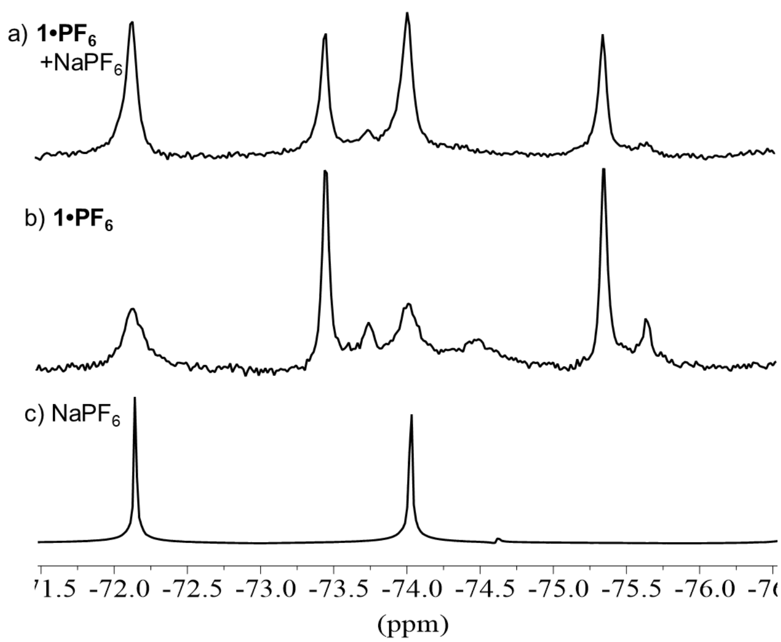

Figure S-16. ^{19}F NMR spectrum of a) **$1•PF_6$** with added $NaPF_6$; b) **$1•PF_6$**; and c) **$NaPF_6$** (D_2O, 376 MHz, 298K). Related to Figure 3 and STAR methods, synthesis of cage **$1•PF_6$**.

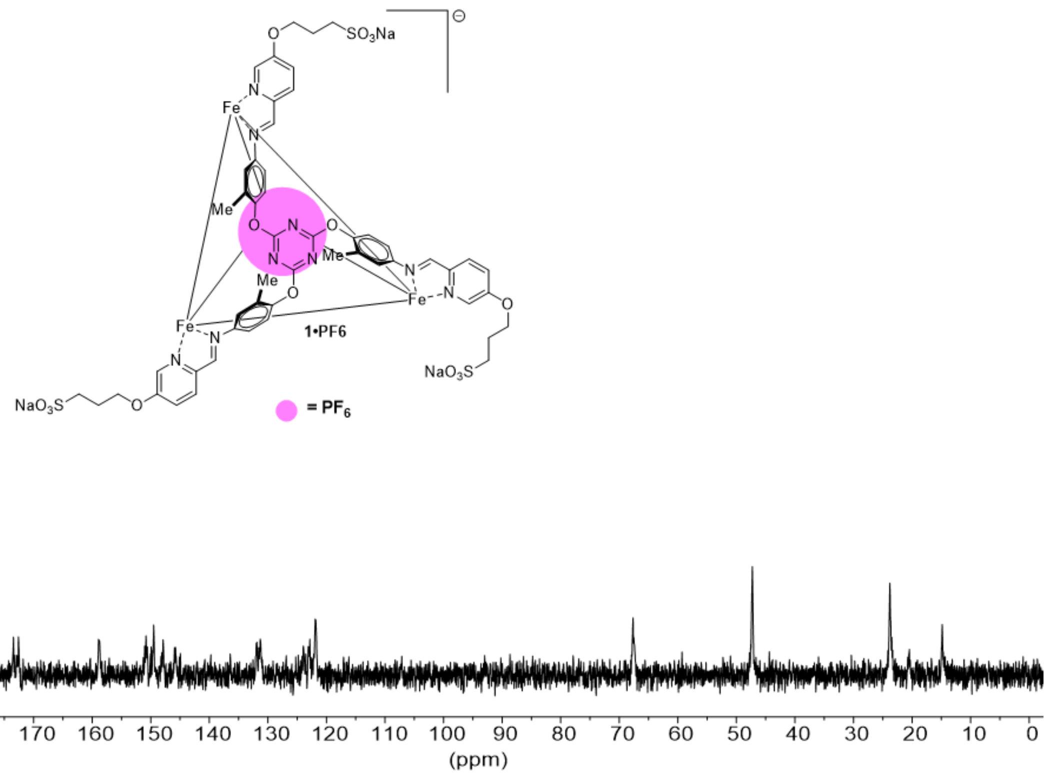

Figure S-17. $^{13}C\{^{1}H\}$ NMR spectrum of cage **1•PF$_6$** (D_2O, 101 MHz, 298K). The low solubility of the complex precluded a high signal to noise ratio in any reasonable amount of time. Related to Figure 1 and STAR methods, synthesis of cage **1•PF$_6$**.

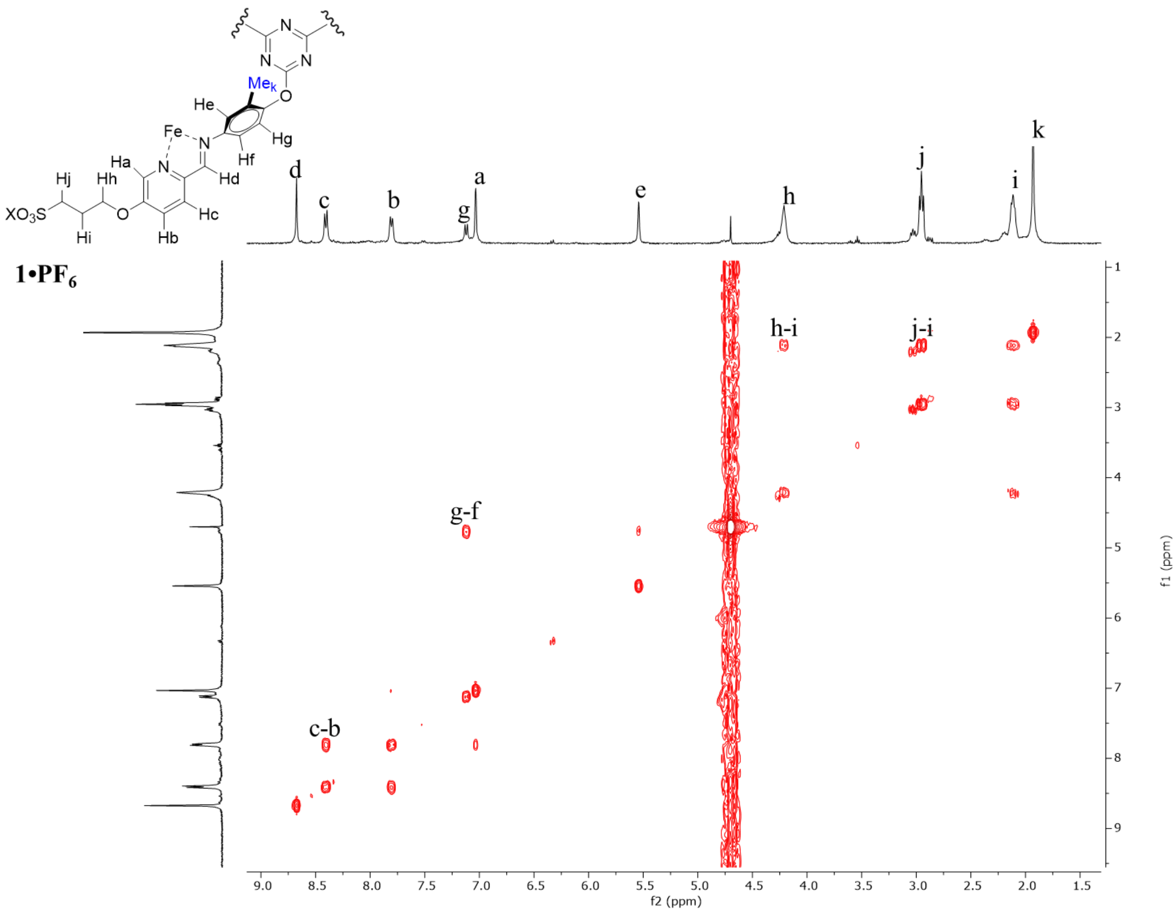

Figure S-18. gCOSY NMR spectrum of cage **1•PF$_6$**. The peak for H_f is under the HDO peak (D_2O, 400 MHz, 298K). Related to Figure 1 and STAR methods, synthesis of cage **1•PF$_6$**.

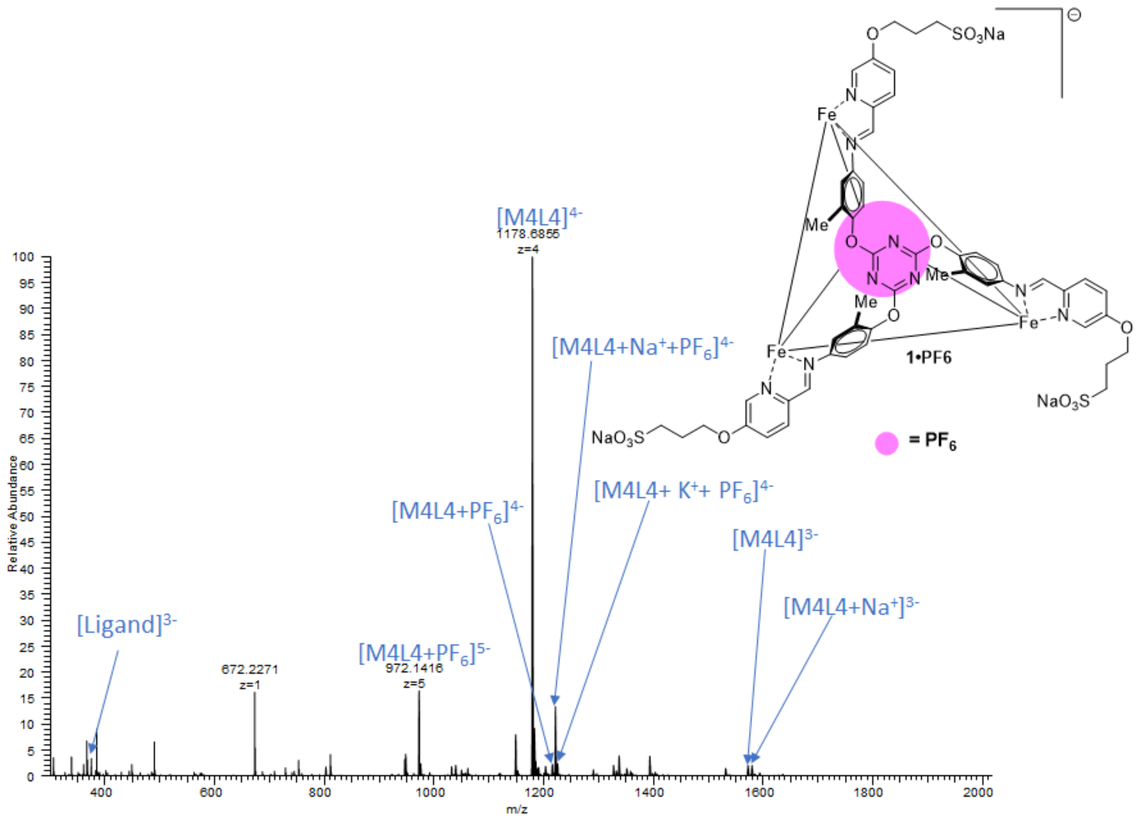

Figure S-19. ESI-MS spectrum of cage **1•PF$_6$.** The flow rate, sheath gas flow rate, aux gas flow rate, spray voltage, capillary temperature, and the S-lens RF level were set to be 3 ul/min, 5 arb, 10 arb, 3.5 kV, 200 C, and 40% respectively. Full mass spectra were acquired with a resolution of r = 30,000. Related to Figure 1 and STAR methods, ESI-MS spectrum of cage **1•PF$_6$**.

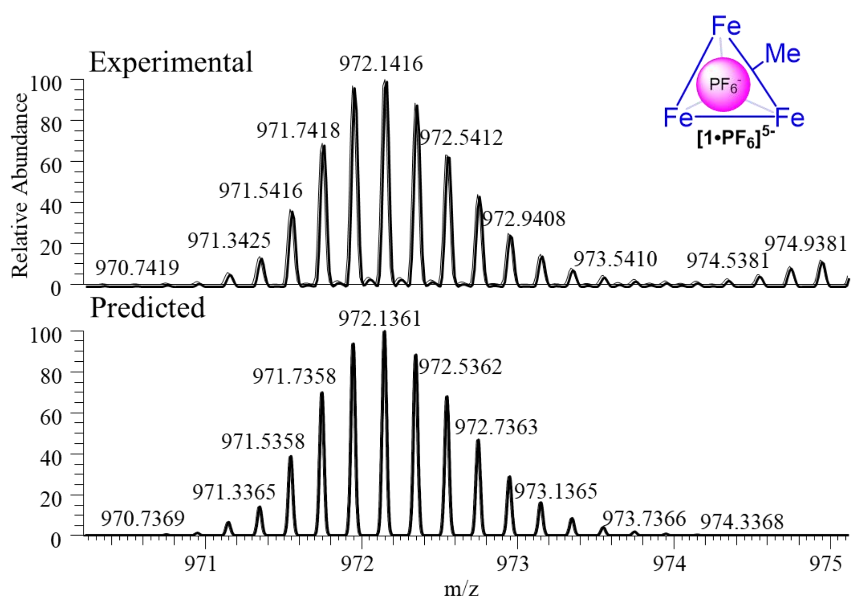

Figure S-20. Expansion of the ESI-MS spectrum of **1•PF$_6$**, showing obtained and simulated isotope region [**1**•PF$_6$]$^{5-}$. Related to Figure 1 and STAR methods, ESI-MS spectrum of cage **1•PF$_6$.**

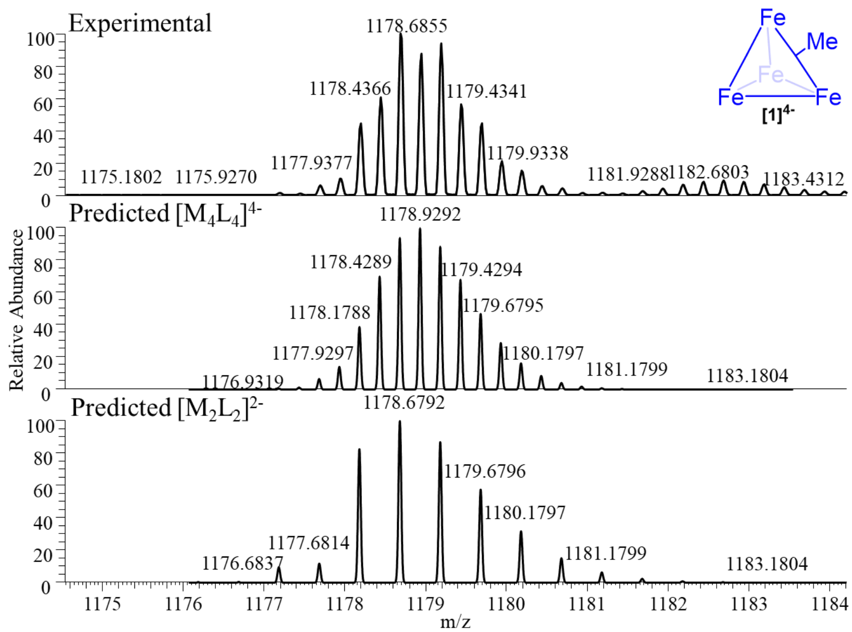

Figure S-21. Expansion of the ESI-MS spectrum of **1•PF$_6$**, showing obtained and simulated isotope region [**1**]$^{4-}$+ [Fe_2L_2]$^{2-}$. Related to Figure 1 and STAR methods, ESI-MS spectrum of cage **1•PF$_6$**.

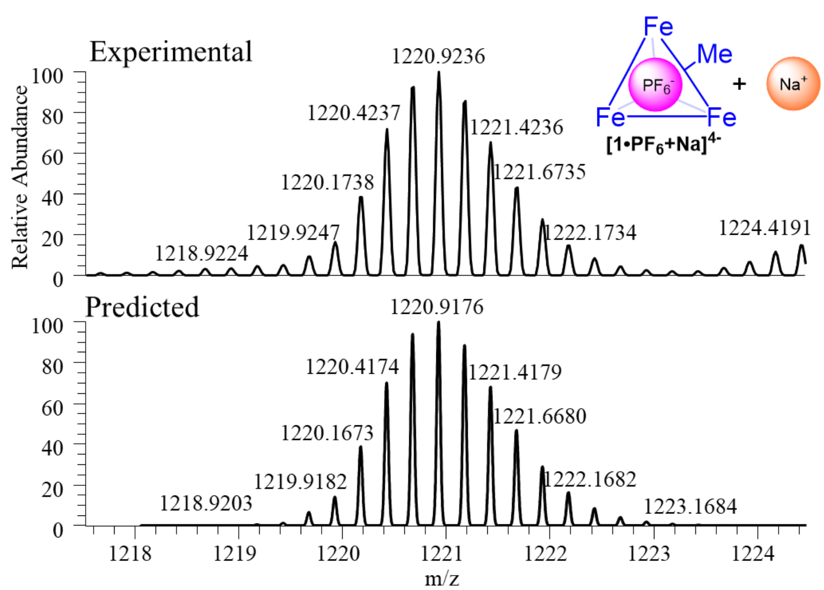

Figure S-22. Expansion of the ESI-MS spectrum of **1•PF$_6$**, showing obtained and simulated isotope region [**1**•PF_6+Na^+]$^{4-}$. Related to Figure 1 and STAR methods, ESI-MS spectrum of cage **1•PF$_6$**.

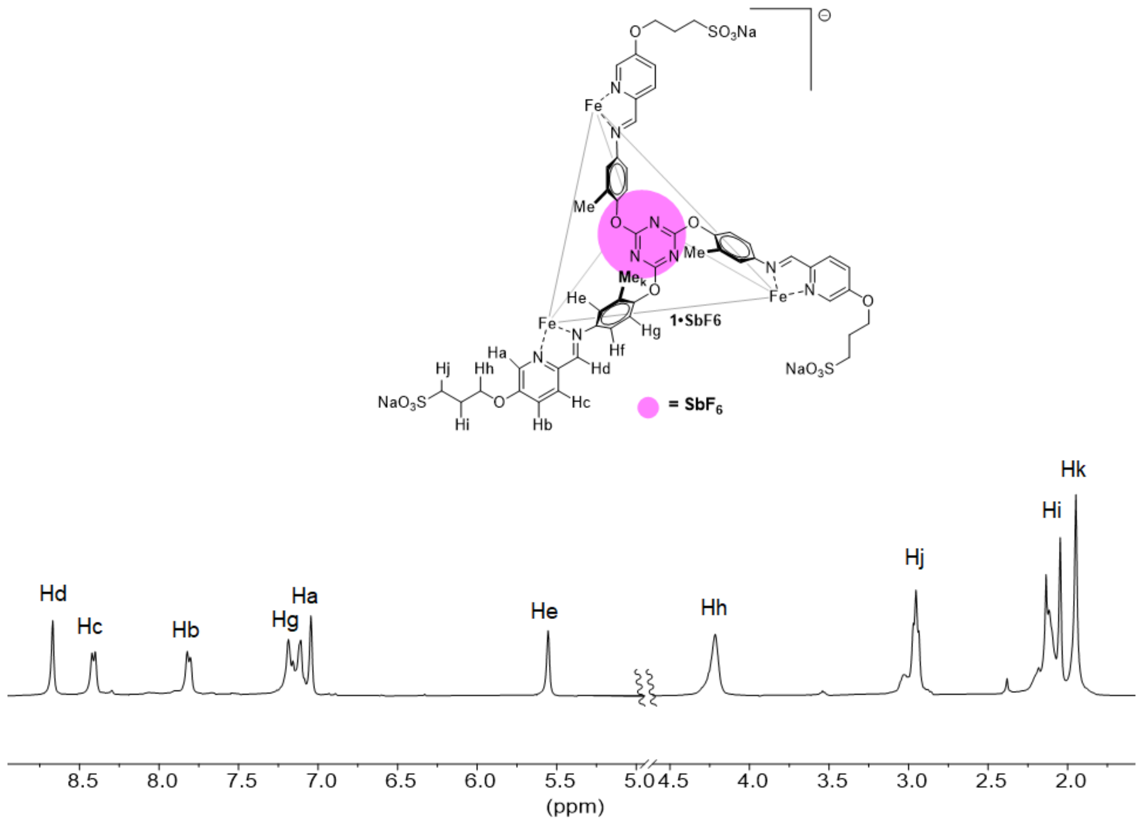

Figure S-23. ^{1}H NMR spectrum of cage **1•SbF₆**. The peak for H_f is under the HDO peak (D_2O, 400 MHz, 298K). Related to Figure 1 and STAR methods, synthesis of cage **1•SbF₆**.

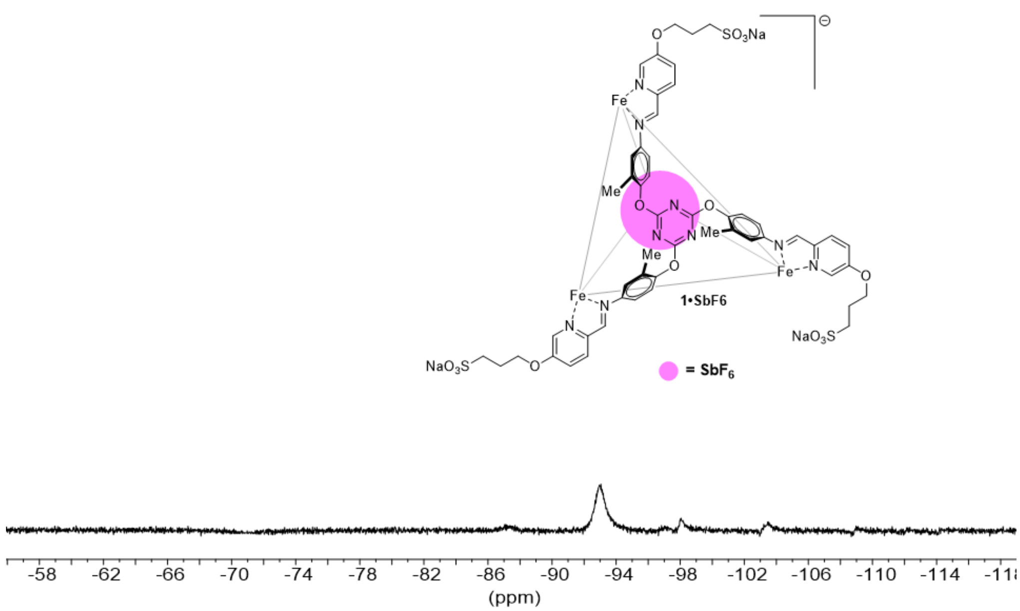

Figure S-24. ^{19}F NMR spectrum of cage **1•SbF₆** (D_2O, 376 MHz, 298K). Related to Figure 1 and STAR methods, synthesis of cage **1•SbF₆**.

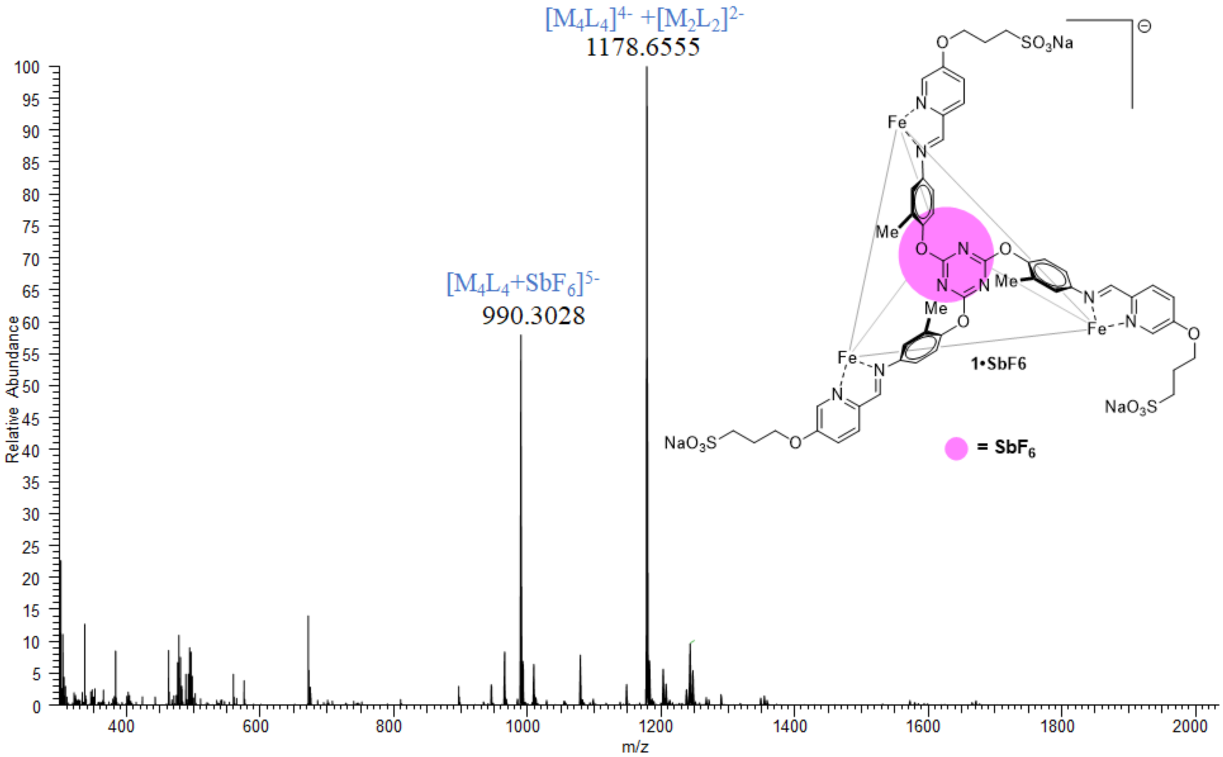

Figure S-25. ESI-MS spectrum of cage **1•SbF$_6$**. The flow rate, sheath gas flow rate, aux gas flow rate, spray voltage, capillary temperature, and the S-lens RF level were set to be 5 ul/min, 5 arb, 10 arb, 4 kV, 200 C, and 20% respectively. Full mass spectra were acquired with a resolution of r = 15,000. Related to Figure 1 and STAR methods, ESI-MS spectrum of cage **1•SbF$_6$**.

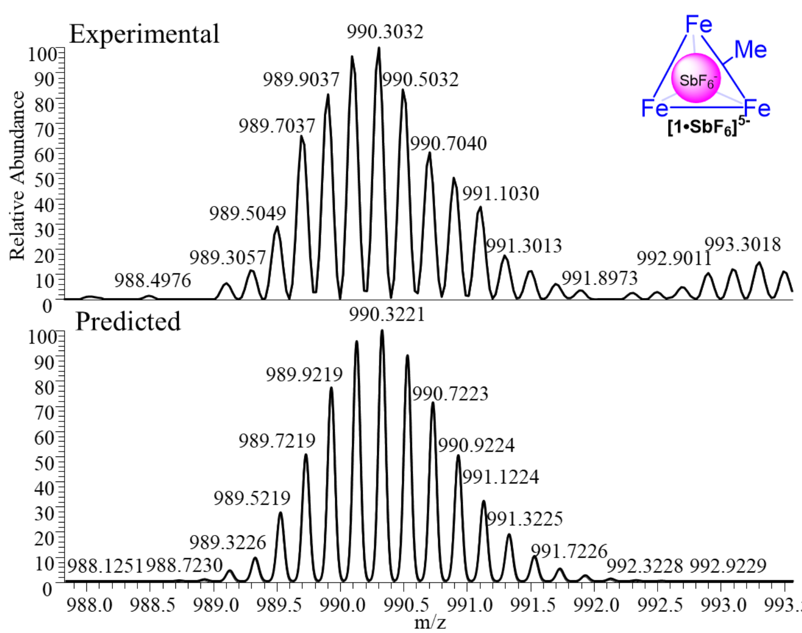

Figure S-26. Expansion of the ESI-MS spectrum of **1•SbF$_6$**, showing obtained and simulated isotope region [**1**•SbF$_6$]$^{5-}$. Related to Figure 1 and STAR methods, ESI-MS spectrum of cage **1•SbF$_6$**.

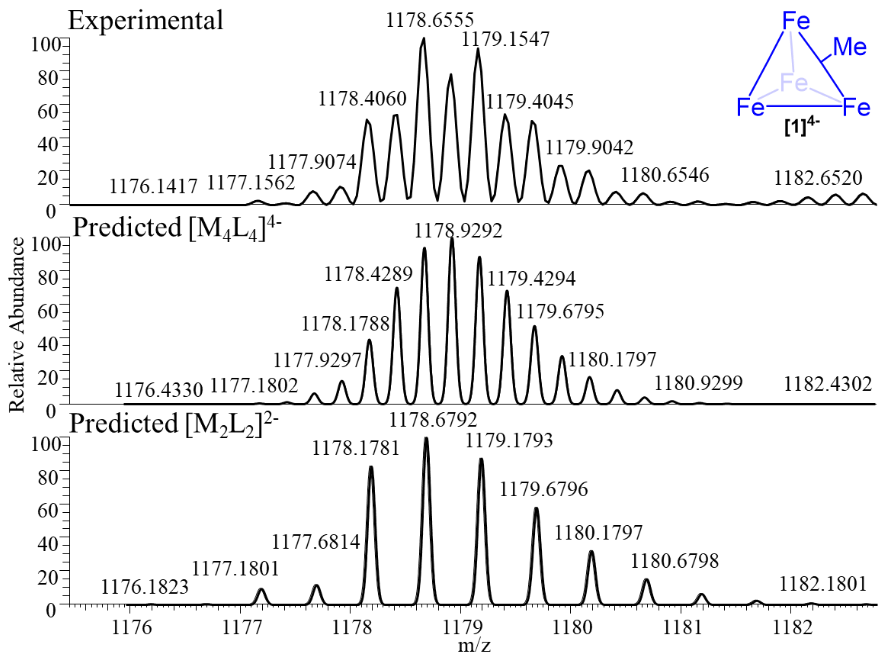

Figure S-27. Expansion of the ESI-MS spectrum of **1•SbF$_6$**, showing obtained and simulated isotope regions [**1**]$^{4-}$+ [Fe$_2$L$_2$]$^{2-}$. Related to Figure 1 and STAR methods, ESI-MS spectrum of cage **1•SbF$_6$**.

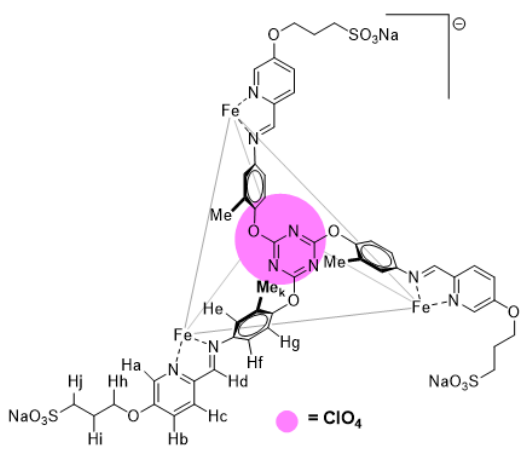

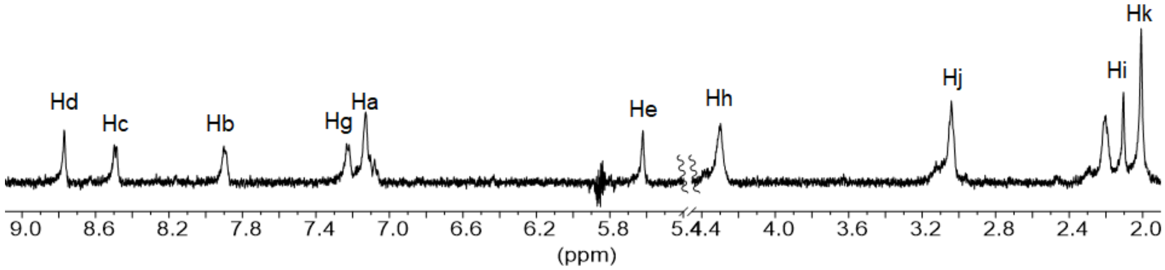

Figure S-28. ^{1}H NMR spectrum of cage **1•ClO$_4$**. The peak for H$_f$ is under the HDO peak (D$_2$O, 600 MHz, 298K). Related to Figure 1 and STAR methods, synthesis of cage **1•ClO$_4$**.

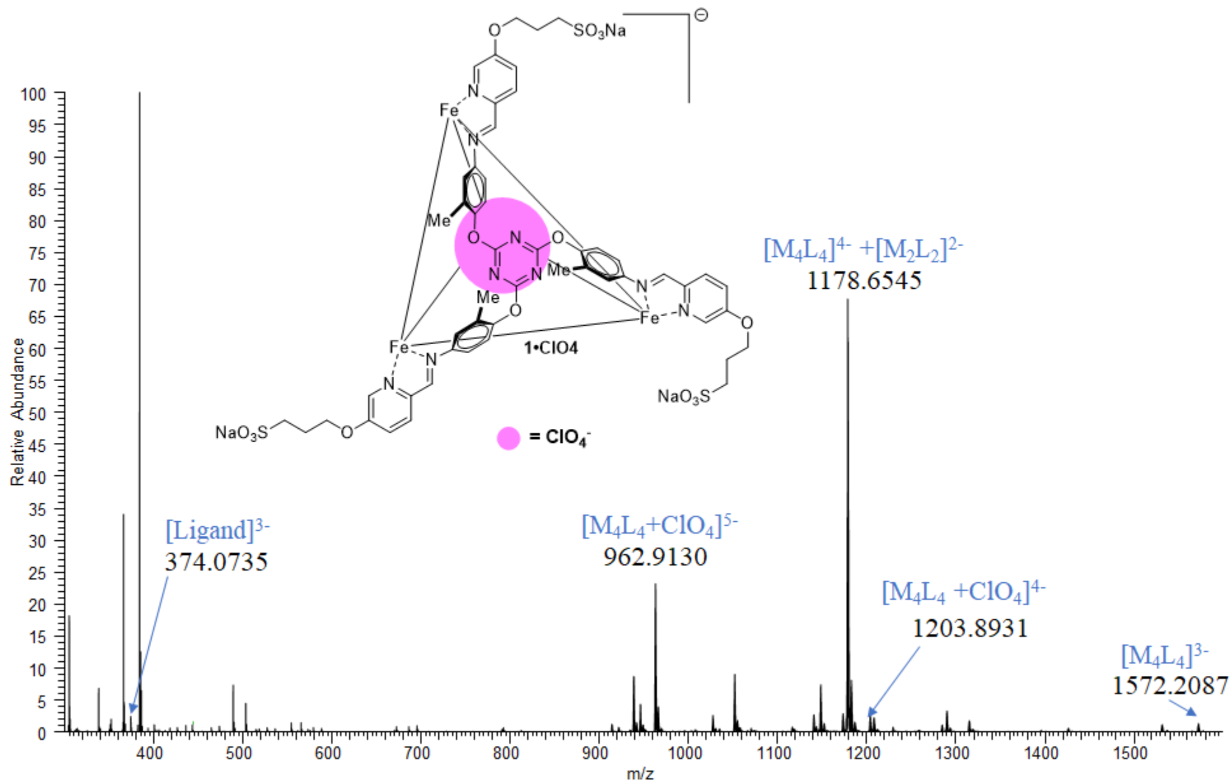

Figure S-29. ESI-MS spectrum of cage **1•ClO₄**. The flow rate, sheath gas flow rate, aux gas flow rate, spray voltage, capillary temperature, and the S-lens RF level were set to be 5 ul/min, 5 arb, 10 arb, 3.5 kV, 200 C, and 20% respectively. Full mass spectra were acquired with a resolution of r = 15,000. Related to Figure 1 and STAR methods, ESI-MS spectrum of cage **1•ClO₄**.

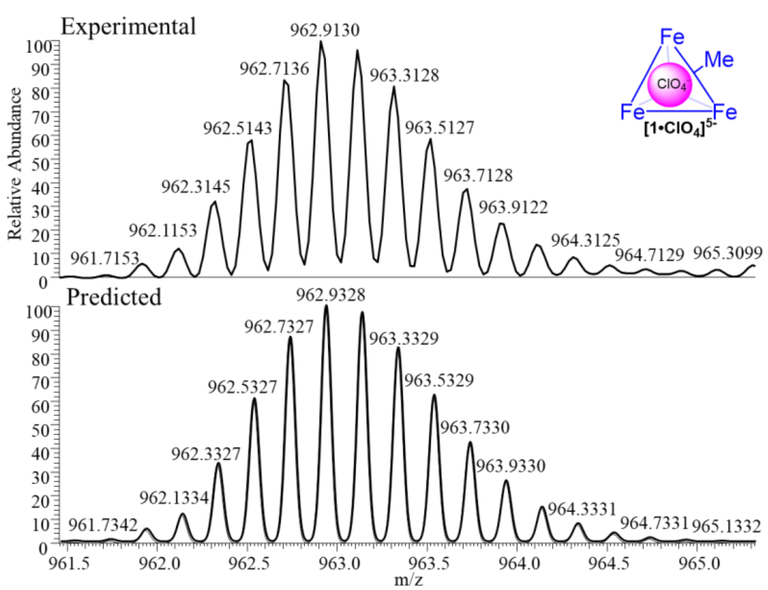

Figure S-30. Expansion of the ESI-MS spectrum of **1•ClO₄**, showing obtained and simulated isotope region [**1**•ClO₄]$^{5-}$. Related to Figure 1 and STAR methods, ESI-MS spectrum of cage **1•ClO₄**.

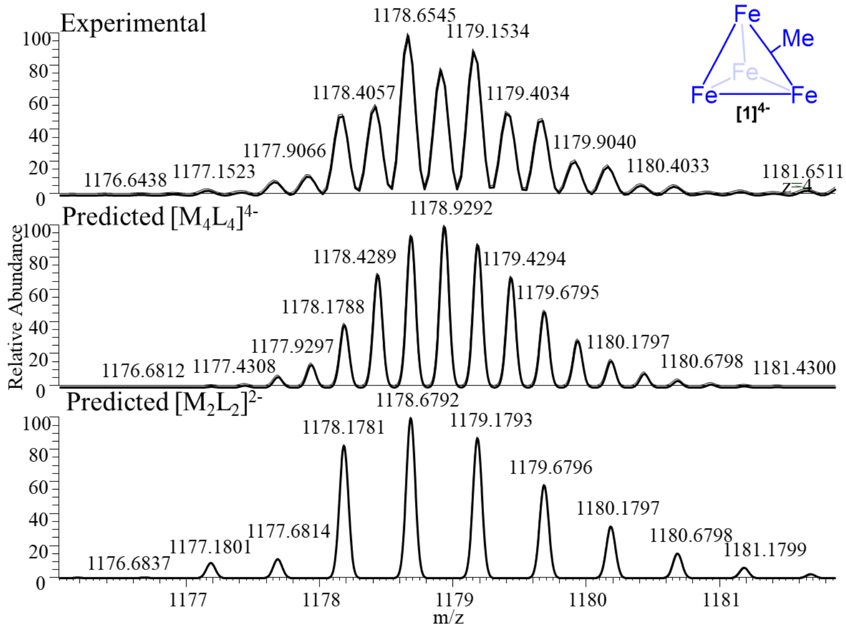

Figure S-31. Expansion of the ESI-MS spectrum of **1•ClO4**, showing obtained and simulated isotope region [**1**]$^{4-}$+ [Fe_2L_2]$^{2-}$. Related to Figure 1 and STAR methods, ESI-MS spectrum of cage **1•ClO4**.

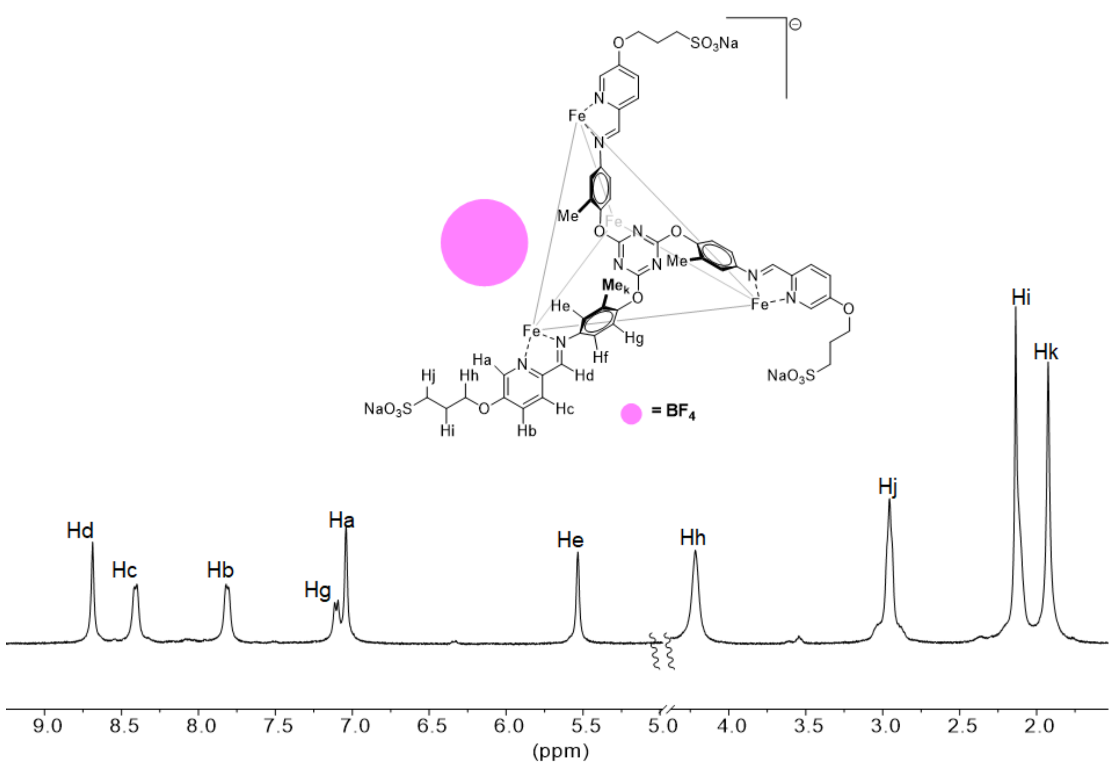

Figure S-32. ^{1}H NMR spectrum of cage **1**, made with $Fe(NTf_2)_2$ and $NaBF_4$. The peak for H_f is under the HDO peak (D_2O, 400 MHz, 298K). Related to Figure 1 and STAR methods, Synthesis of **1**, made with $Fe(NTf_2)_2$ and $NaBF_4$.

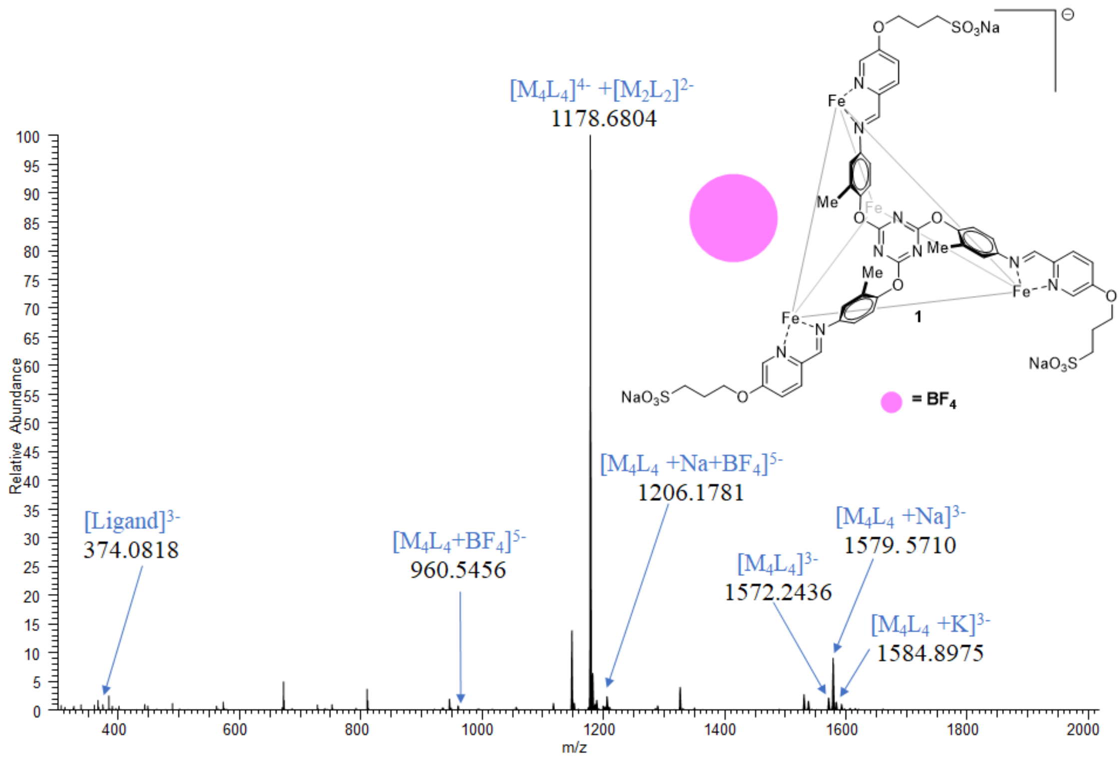

Figure S-33. ESI-MS spectrum of cage **1**, made with $Fe(NTf_2)_2$ and $NaBF_4$. The flow rate, sheath gas flow rate, aux gas flow rate, spray voltage, capillary temperature, and the S-lens RF level were set to be 3 ul/min, 5 arb, 10 arb, 3.2 kV, 200 C, and 40% respectively. Full mass spectra were acquired with a resolution of r = 30,000. Related to Figure 1 and STAR methods, ESI-MS spectrum of cage **1**, made with $Fe(NTf_2)_2$ and $NaBF_4$.

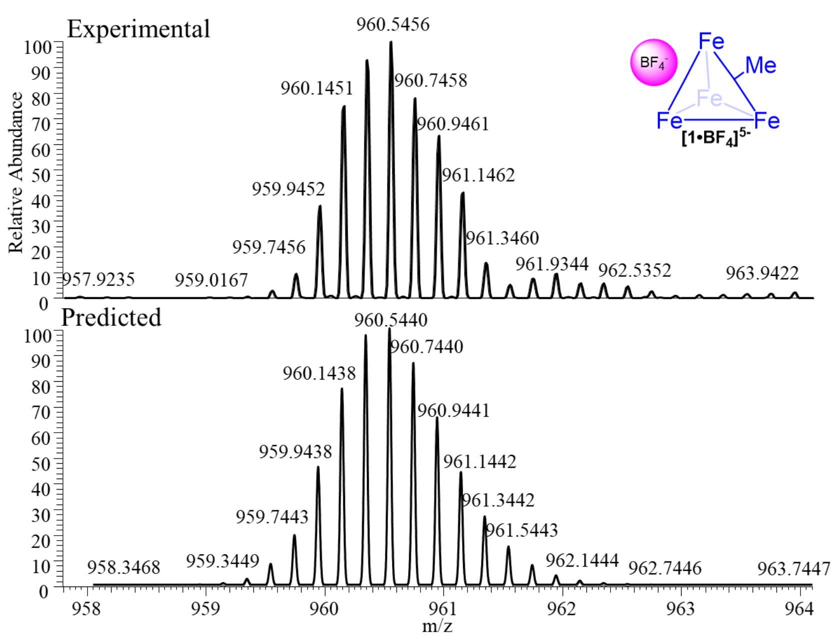

Figure S-34. Expansion of the ESI-MS spectrum of **1**, made with $Fe(NTf_2)_2$ and $NaBF_4$, showing obtained and simulated isotope region [**1** + BF_4]$^{5-}$. Related to Figure 1 and STAR methods, ESI-MS spectrum of cage **1**, made with $Fe(NTf_2)_2$ and $NaBF_4$.

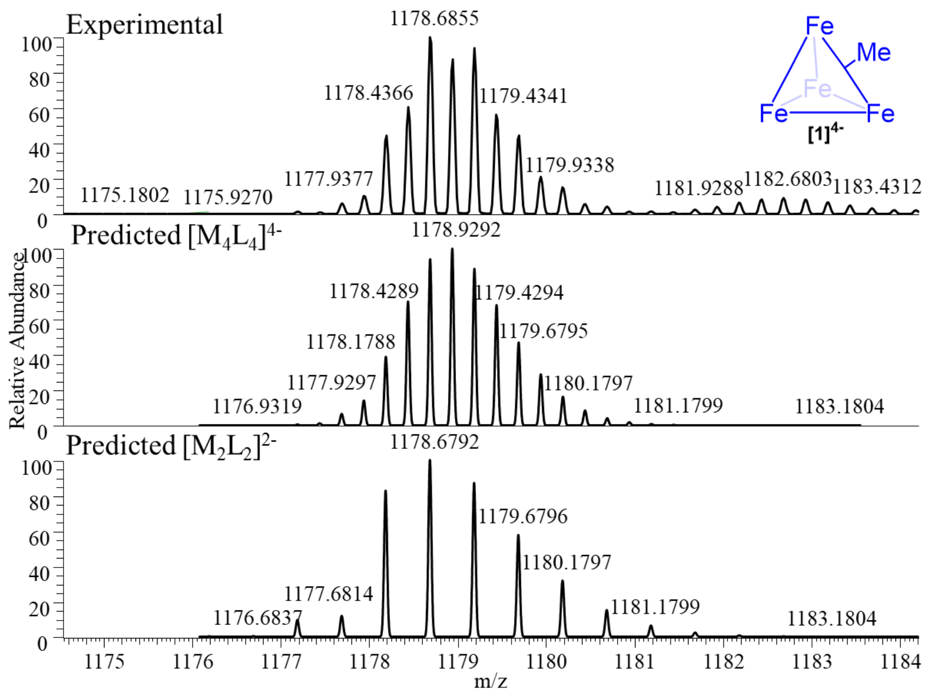

Figure S-35. Expansion of the ESI-MS spectrum of **1**, made with $Fe(NTf_2)_2$ and $NaBF_4$, showing obtained and simulated isotope region $[\mathbf{1}]^{4-}$+ $[Fe_2L_2]^{2-}$. Related to Figure 1 and STAR methods, ESI-MS spectrum of cage **1**, made with $Fe(NTf_2)_2$ and $NaBF_4$.

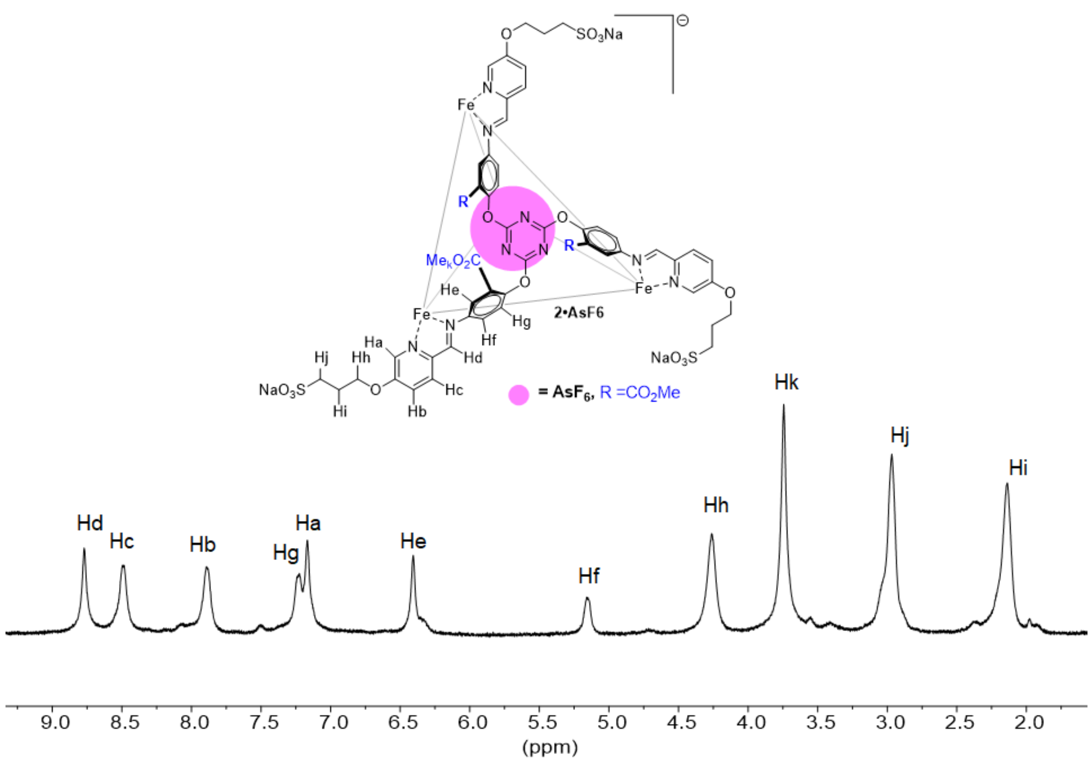

Figure S-36. ^{1}H NMR spectrum of cage **2•AsF$_6$** (D_2O, 400 MHz, 298K). Related to Figure 1 and STAR methods, Synthesis of cage **2•AsF$_6$.**

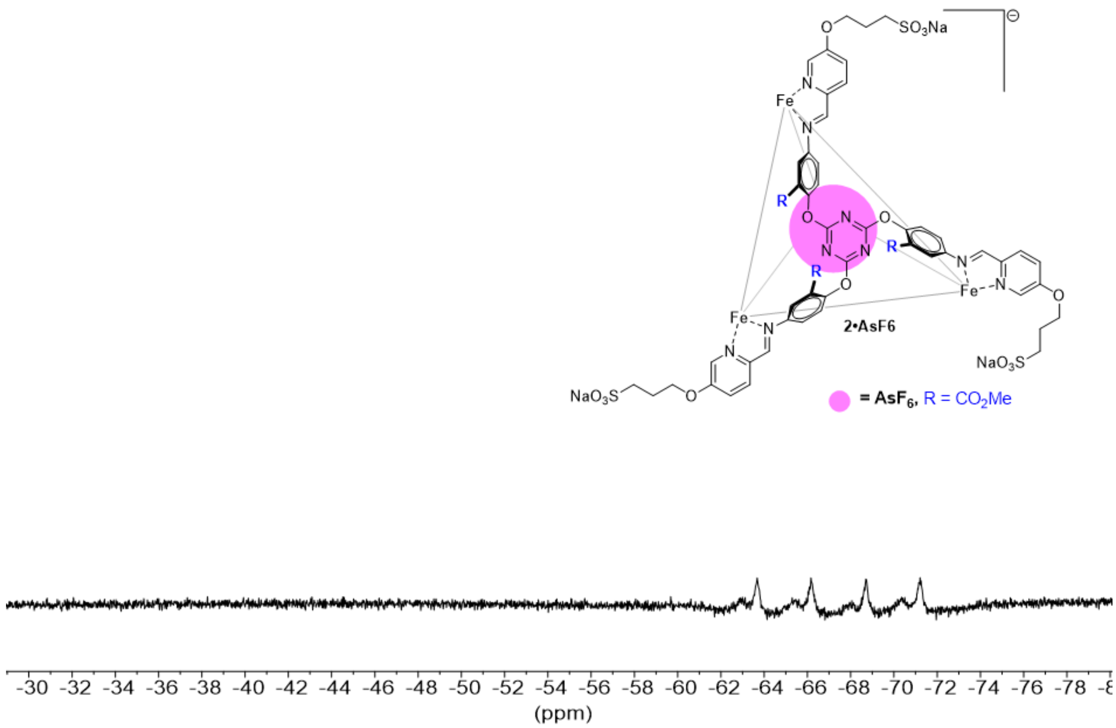

Figure S-37. ^{19}F NMR spectrum of cage **2•AsF$_6$** (D_2O, 376 MHz, 298K). Related to Figure 1 and STAR methods, Synthesis of cage **2•AsF$_6$.**

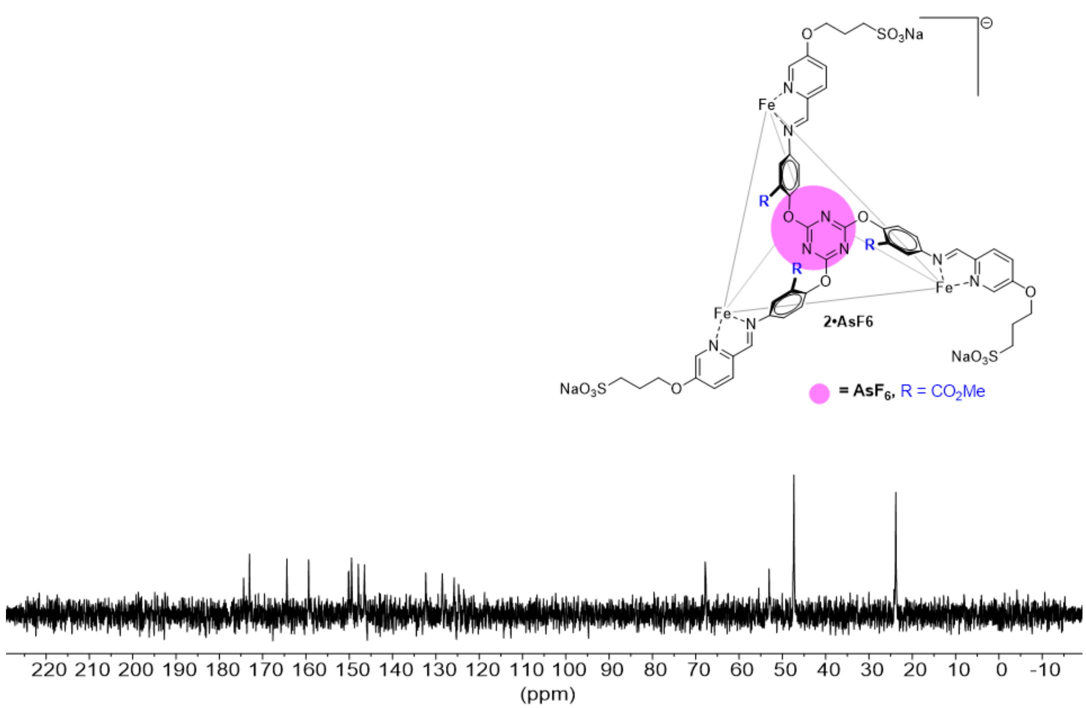

Figure S-38. $^{13}C\{^1H\}$ NMR spectrum of cage **2•AsF$_6$** (D_2O, 101 MHz, 298K). The low solubility of the complex precluded a high signal to noise ratio in any reasonable amount of time. Related to Figure 1 and STAR methods, Synthesis of cage **2•AsF$_6$.**

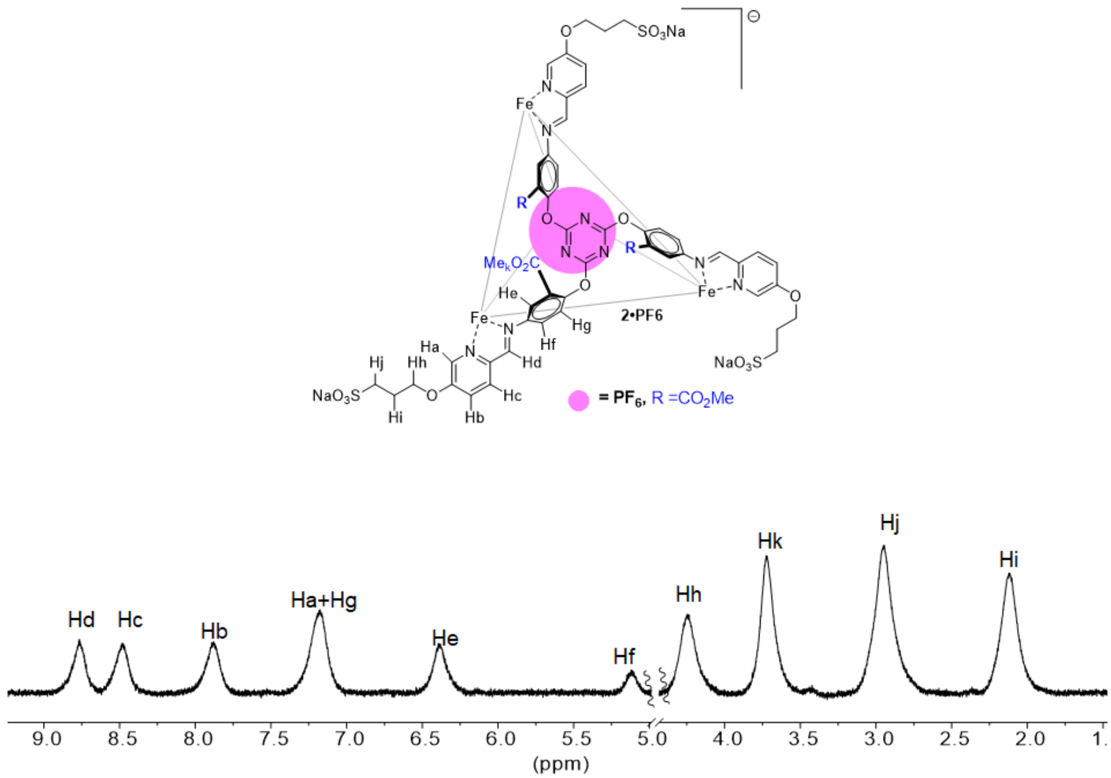

Figure S-39. ^{1}H NMR spectrum of cage **2•PF$_6$** (D_2O, 400 MHz, 298K). Related to Figure 1 and STAR methods, Synthesis of cage **2•PF$_6$.**

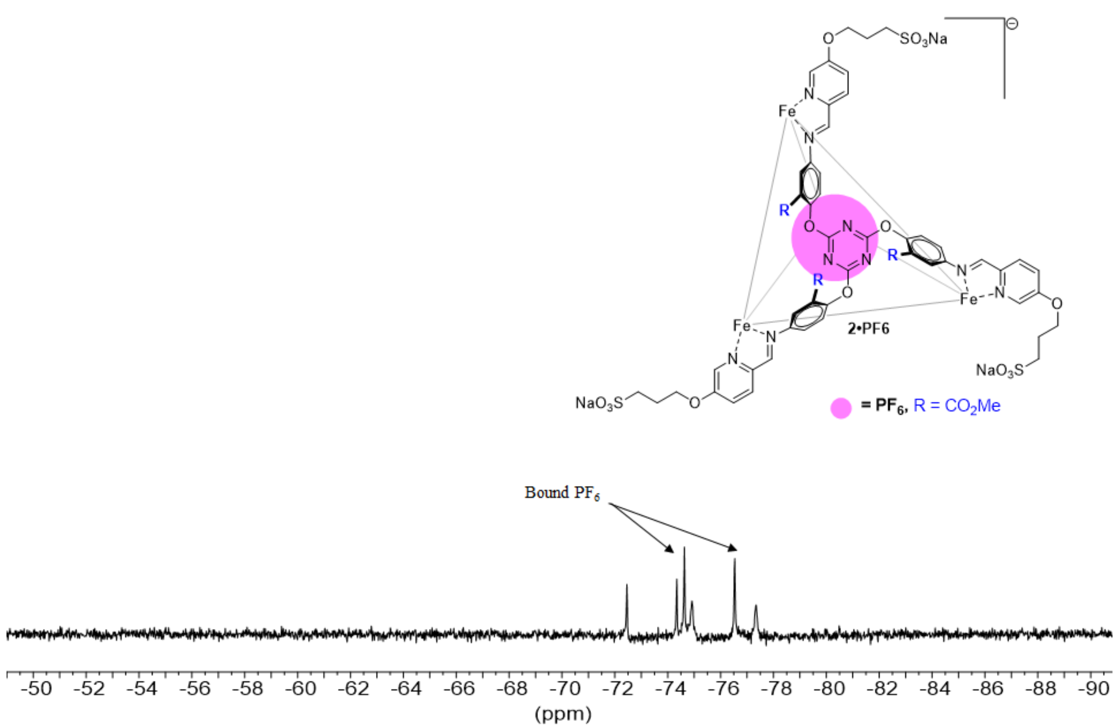

Figure S-40. ^{19}F NMR spectrum of cage **2•PF$_6$** (D_2O, 376 MHz, 298K). Related to Figure 1 and STAR methods, Synthesis of cage **2•PF$_6$.**

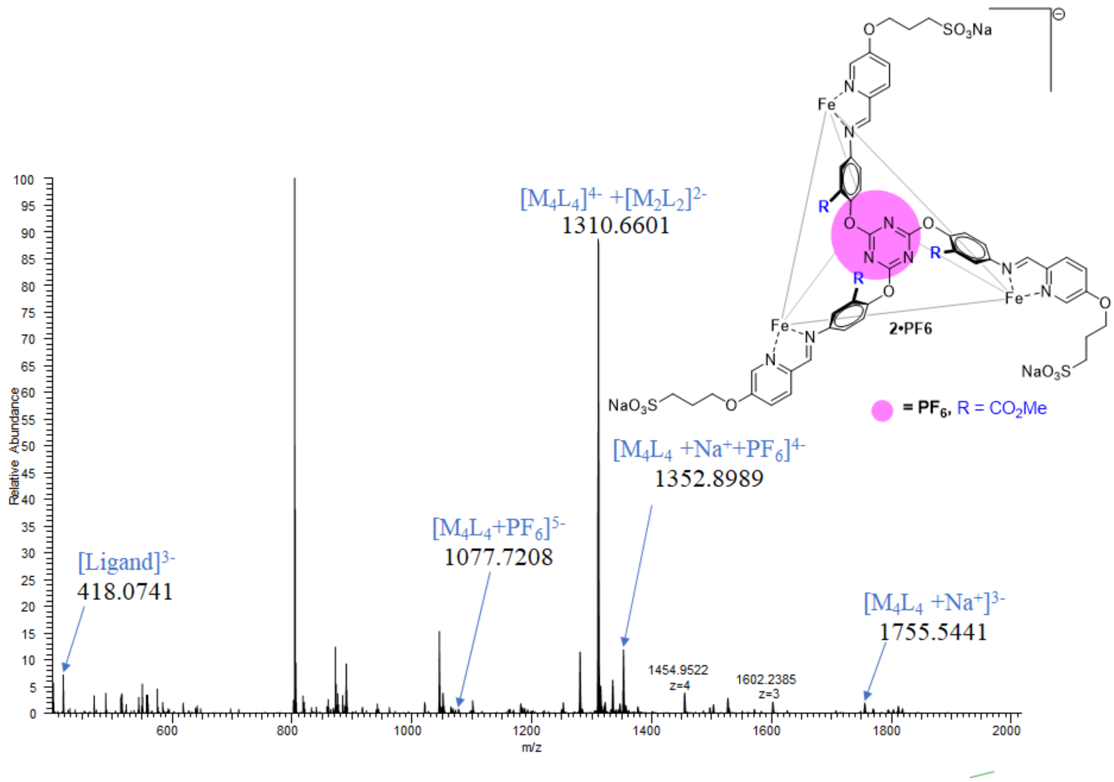

Figure S-41. ESI-MS spectrum of cage **2•PF$_6$**. The flow rate, sheath gas flow rate, aux gas flow rate, spray voltage, capillary temperature, and the S-lens RF level were set to be 3 ul/min, 5 arb, 10 arb, 3.5 kV, 200 C, and 50% respectively. Full mass spectra were acquired with a resolution of r = 30,000. Related to Figure 1 and STAR methods, ESI-MS spectrum of cage **2•PF$_6$.**

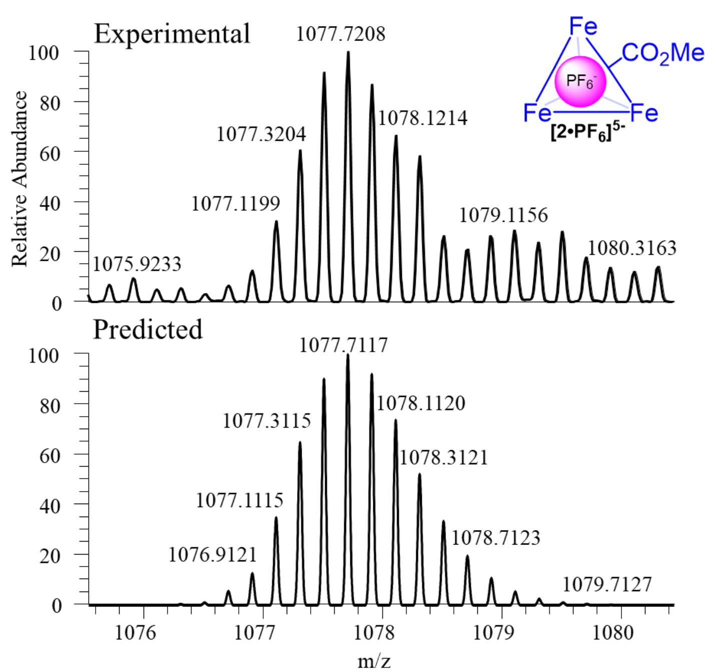

Figure S-42. Expansion of the ESI-MS spectrum of **2•PF$_6$**, showing obtained and simulated isotope region [**2**•PF$_6$]$^{5-}$. Related to Figure 1 and STAR methods, ESI-MS spectrum of cage **2•PF$_6$.**

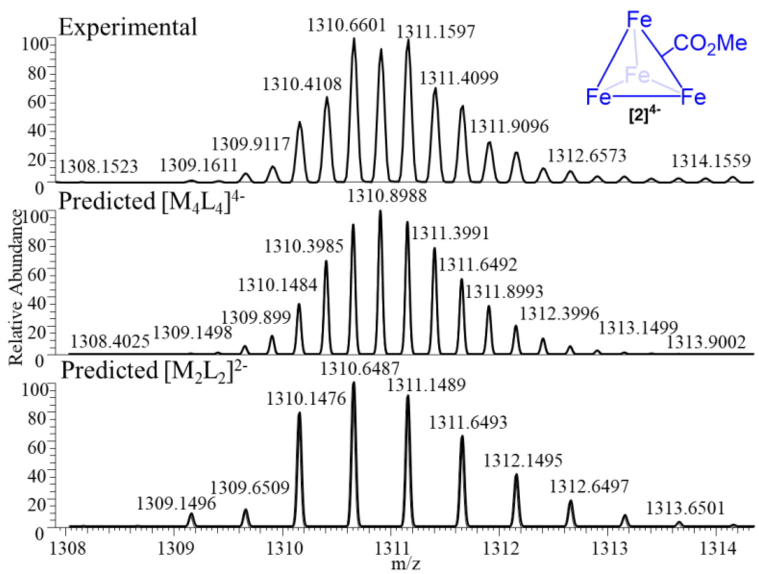

Figure S-43. Expansion of the ESI-MS spectrum of **2•PF₆**, showing obtained and simulated isotope region [**2**]$^{4-}$+ [Fe_2L_2]$^{2-}$. Related to Figure 1 and STAR methods, ESI-MS spectrum of cage **2•PF₆.**

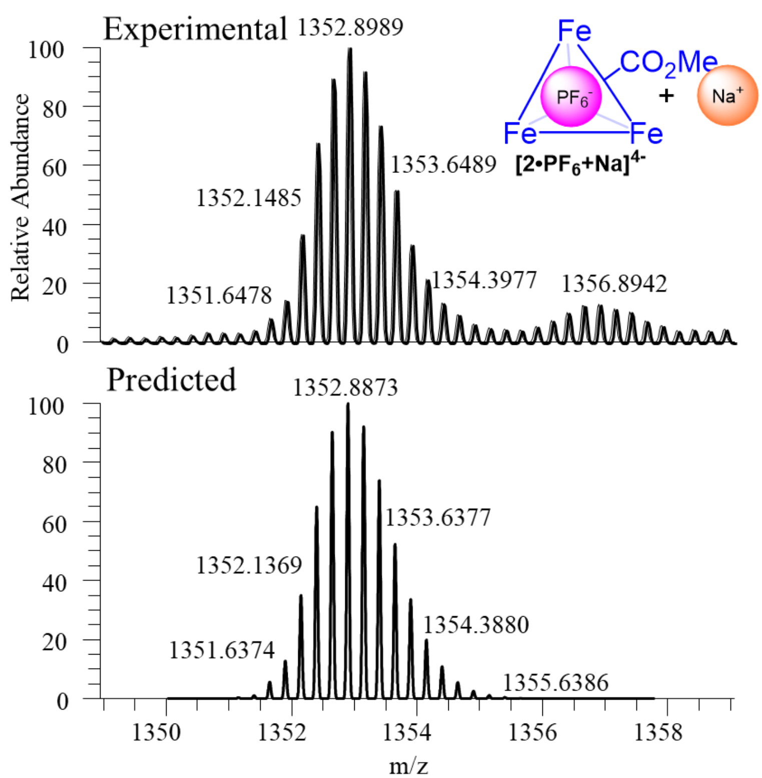

Figure S-44*.* Expansion of the ESI-MS spectrum of **2•PF₆**, showing obtained and simulated isotope region [**2**•PF_6+Na^+]$^{4-}$. Related to Figure 1 and STAR methods, ESI-MS spectrum of cage **2•PF₆.**

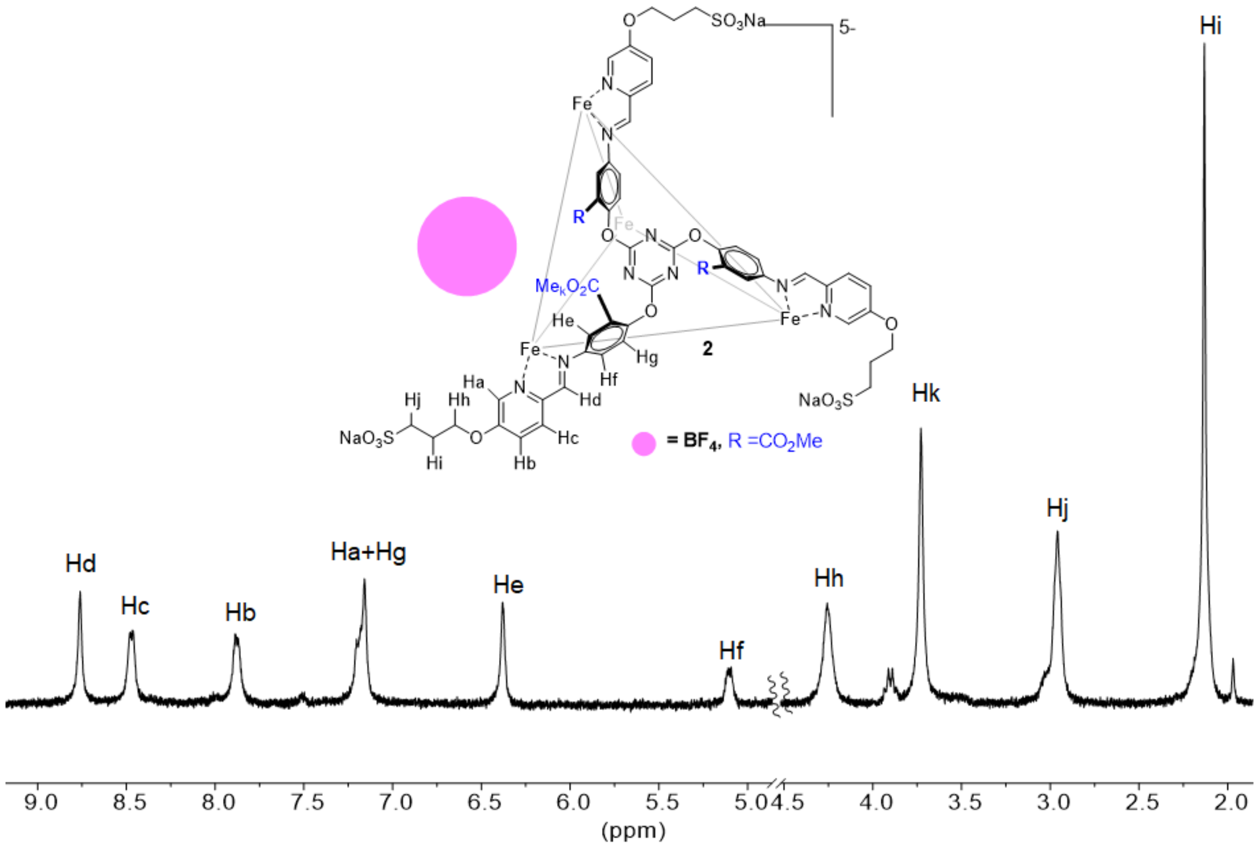

Figure S-45. ^{1}H NMR spectrum of cage **2**, made with $Fe(NTf_2)_2$ and $NaBF_4$ (D_2O, 400 MHz, 298K). Related to Figure 1 and STAR methods, Synthesis of **2**, made with $Fe(NTf_2)_2$ and $NaBF_4$.

Anion Recognition: Binding in Unoccupied Cages

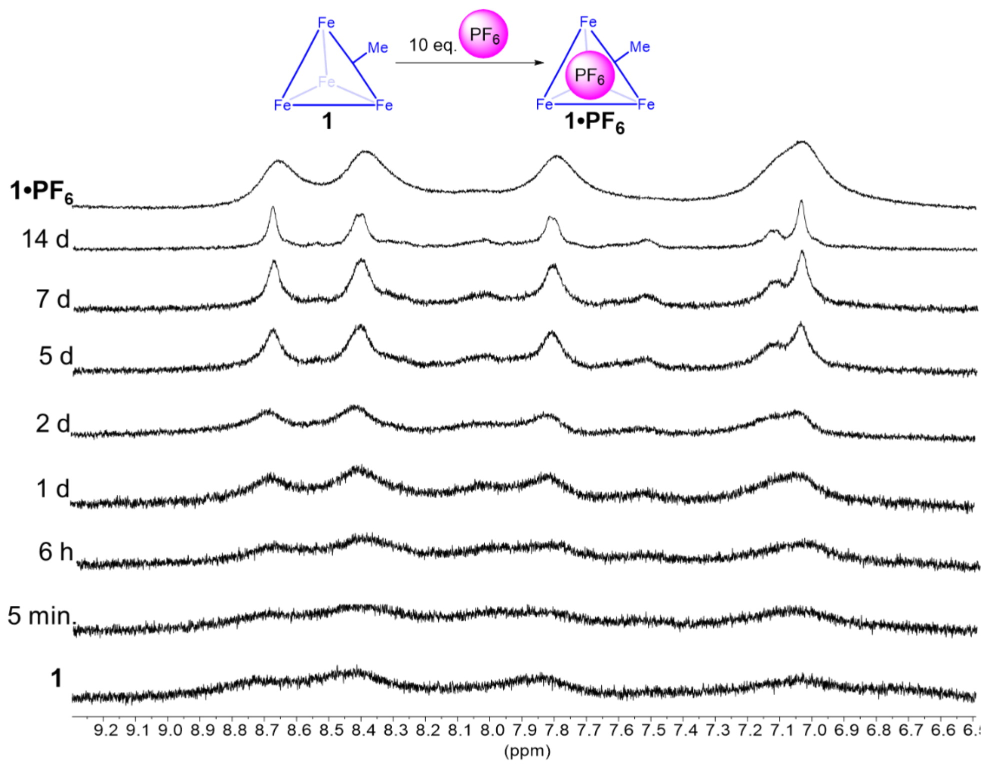

Figure S-46. [1]H NMR spectra of **1** with 10 equivalents of $NaPF_6$ added, over 14 days (D_2O, 400 MHz, 298K). Related to Figure 5.

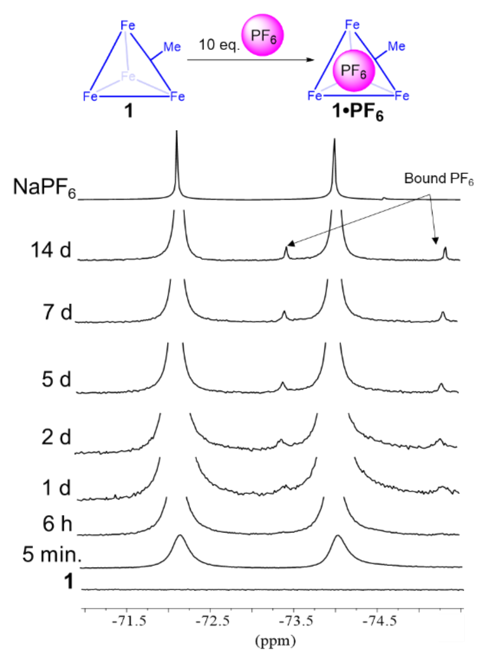

Figure S-47. [19]F NMR spectra of **1** with 10 equivalents of $NaPF_6$ added, over 14 d (D_2O, 376 MHz, 298K). Related to Figure 5.

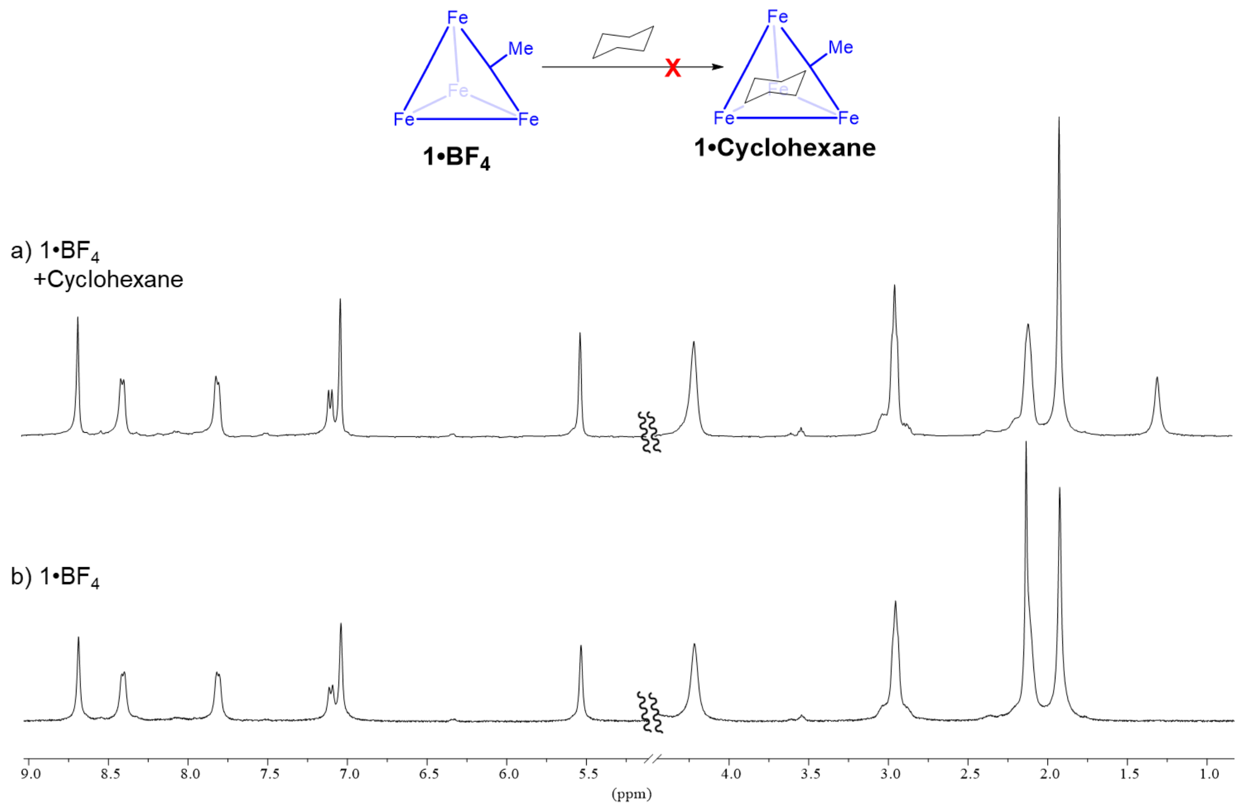

Figure S-48. ^{1}H NMR spectrum of a) **1**, made with $Fe(NTf_2)_2$ and $NaBF_4$ with 10 equivalents of cyclohexane added and b) **1•BF$_4$** (D_2O, 400 MHz, 298K). Related to Figure 7.

Anion Recognition: Anion Exchange Experiments in Occupied Cages

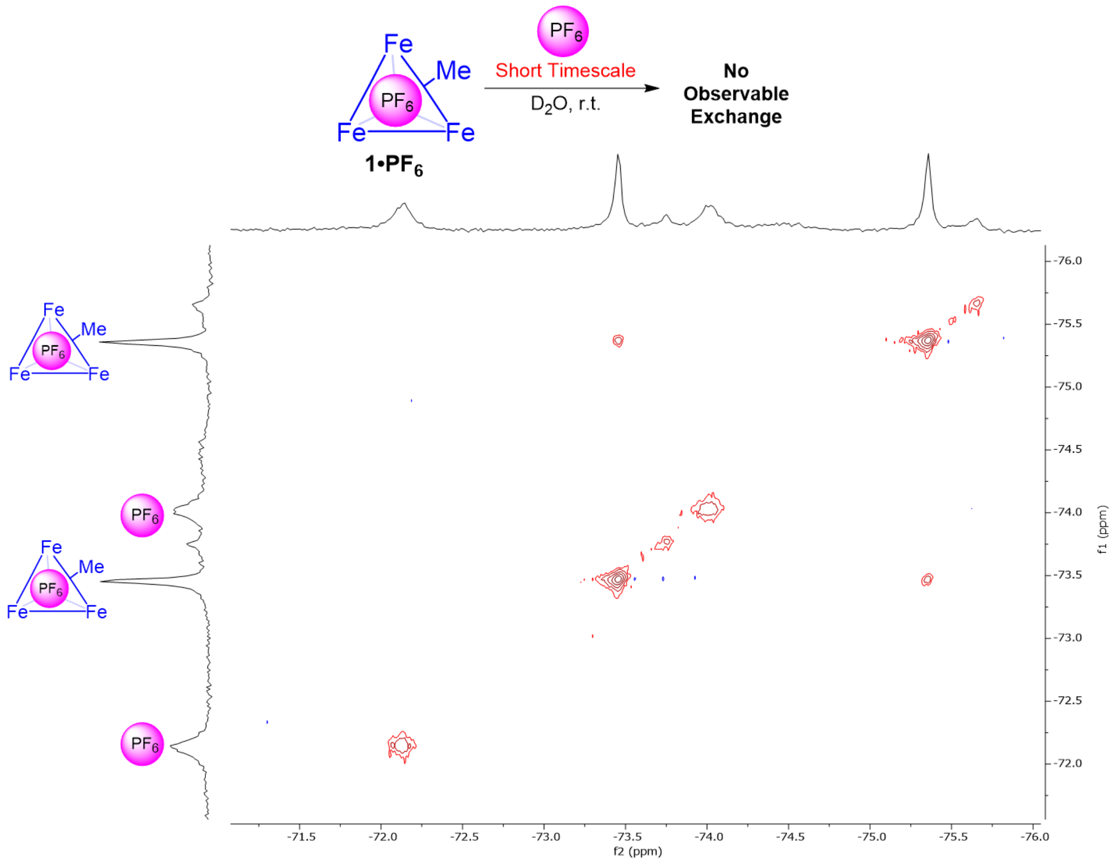

Figure S-49. ^{19}F-^{19}F EXSY NMR spectrum of **1•PF₆** (2 mM, D_2O, 376 MHz, 300 ms mixing time, 298K). Related to Figure 4.

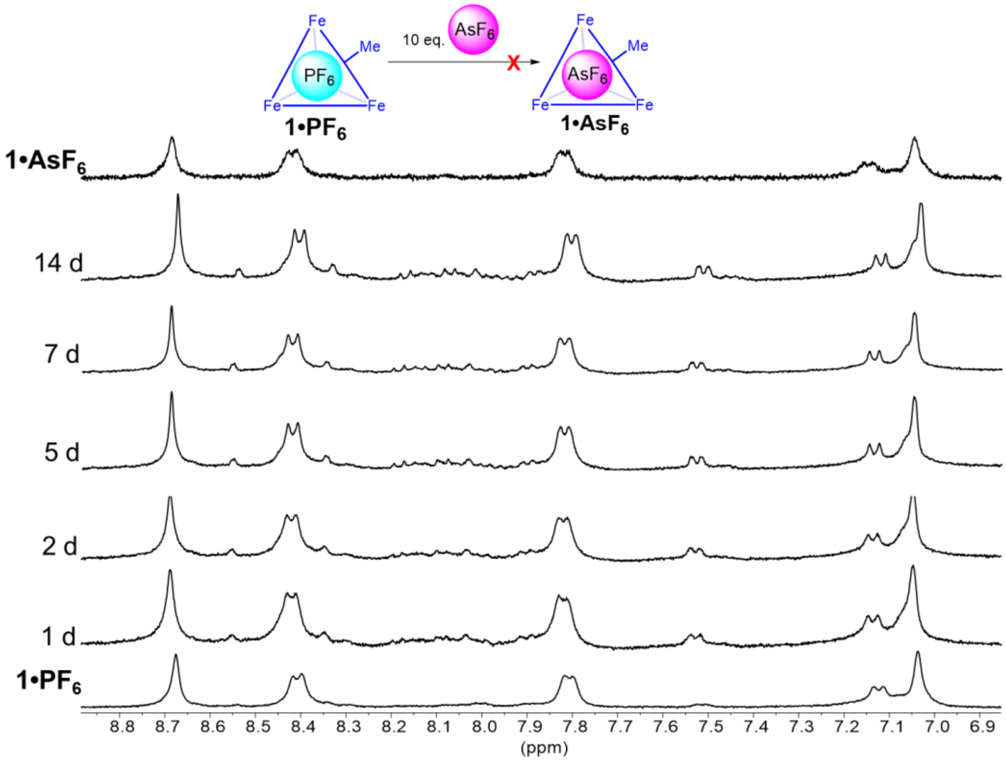

Figure S-50. [1]H NMR spectra of **1•PF$_6$** with 10 equivalents of NaAsF$_6$, over 14 days (D_2O, 400 MHz, 298K). Related to Figure 4.

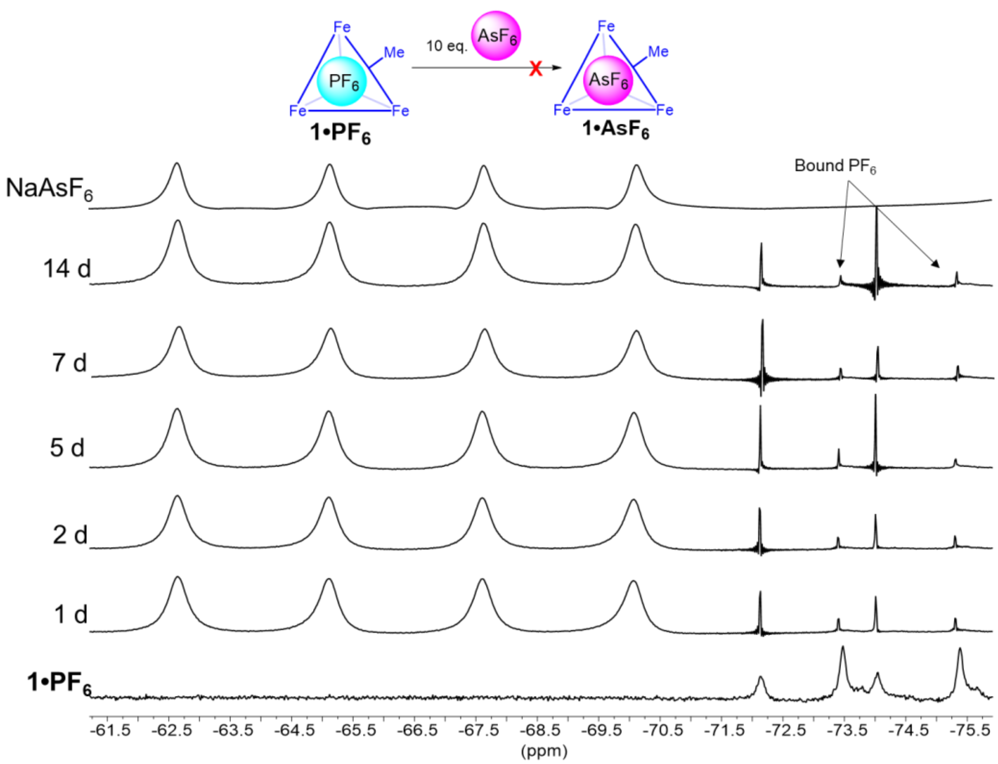

Figure S-51. [19]F NMR spectra of **1•PF$_6$** with 10 equivalents of NaAsF$_6$, over 14 days (D_2O, 376 MHz, 298K). Related to Figure 4.

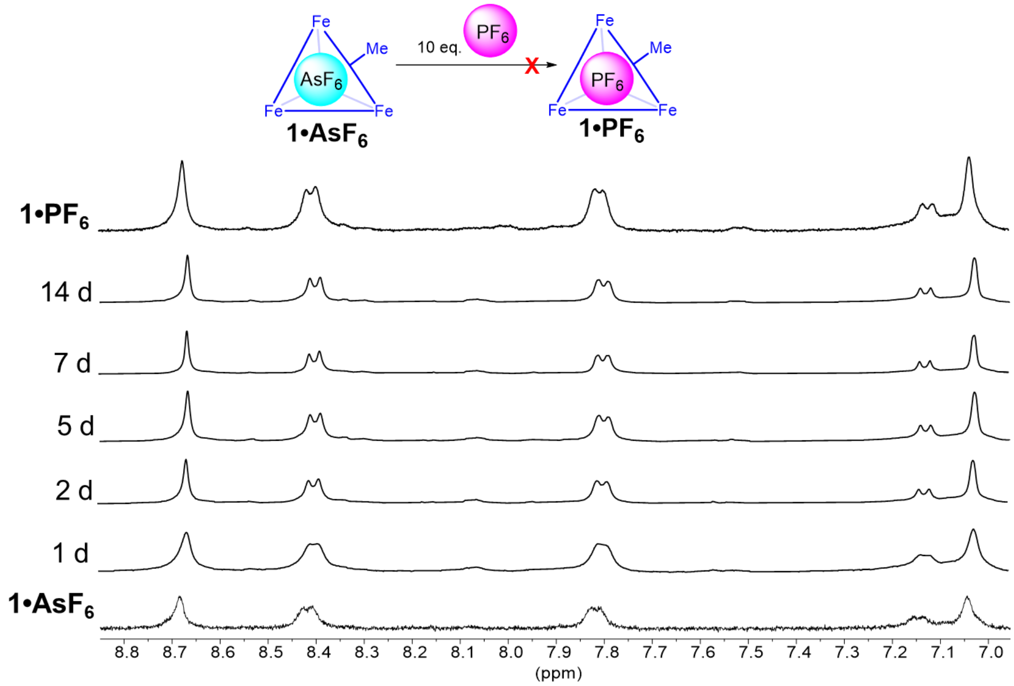

Figure S-52. [1]H NMR spectra of **1•AsF$_6$** with 10 equivalents of NaPF$_6$, over 14 days (D$_2$O, 400 MHz, 298K). Related to Figure 4.

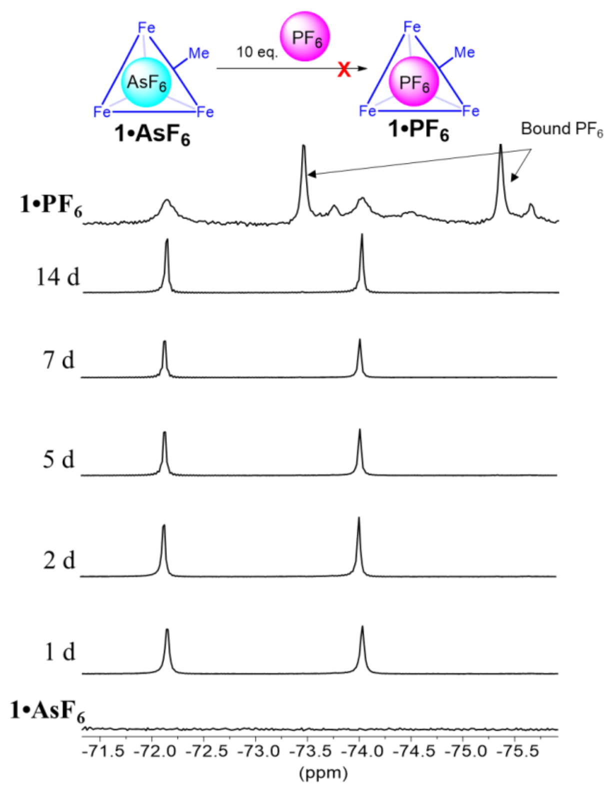

Figure S-53. [19]F NMR spectra of **1•AsF$_6$** with 10 equivalents of NaPF$_6$, over 14 days (D$_2$O, 376 MHz, 298K). Related to Figure 4.

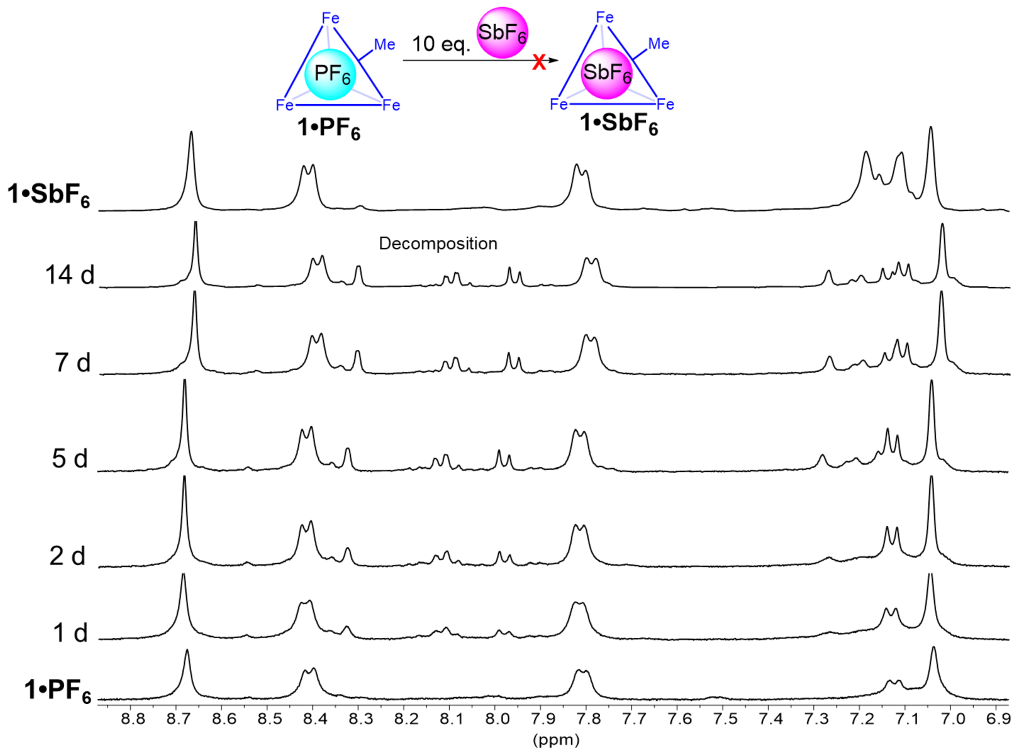

Figure S-54. ^{1}H NMR spectra of **1•PF$_6$** with 10 equivalents of $NaSbF_6$, over 14 days (D_2O, 400 MHz, 298 K). Related to Figure 7.

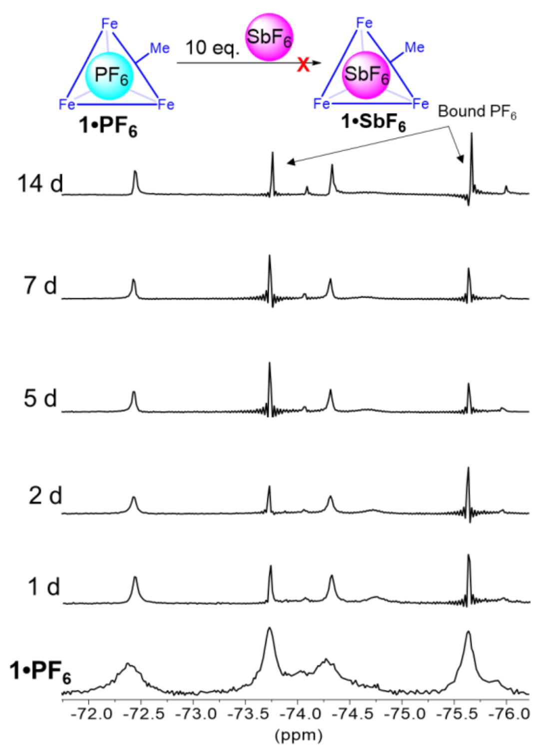

Figure S-55. ^{19}F NMR spectra of **1•PF$_6$** with 10 equivalents of $NaSbF_6$, over 14 days (D_2O, 376 MHz, 298K). Related to Figure 7.

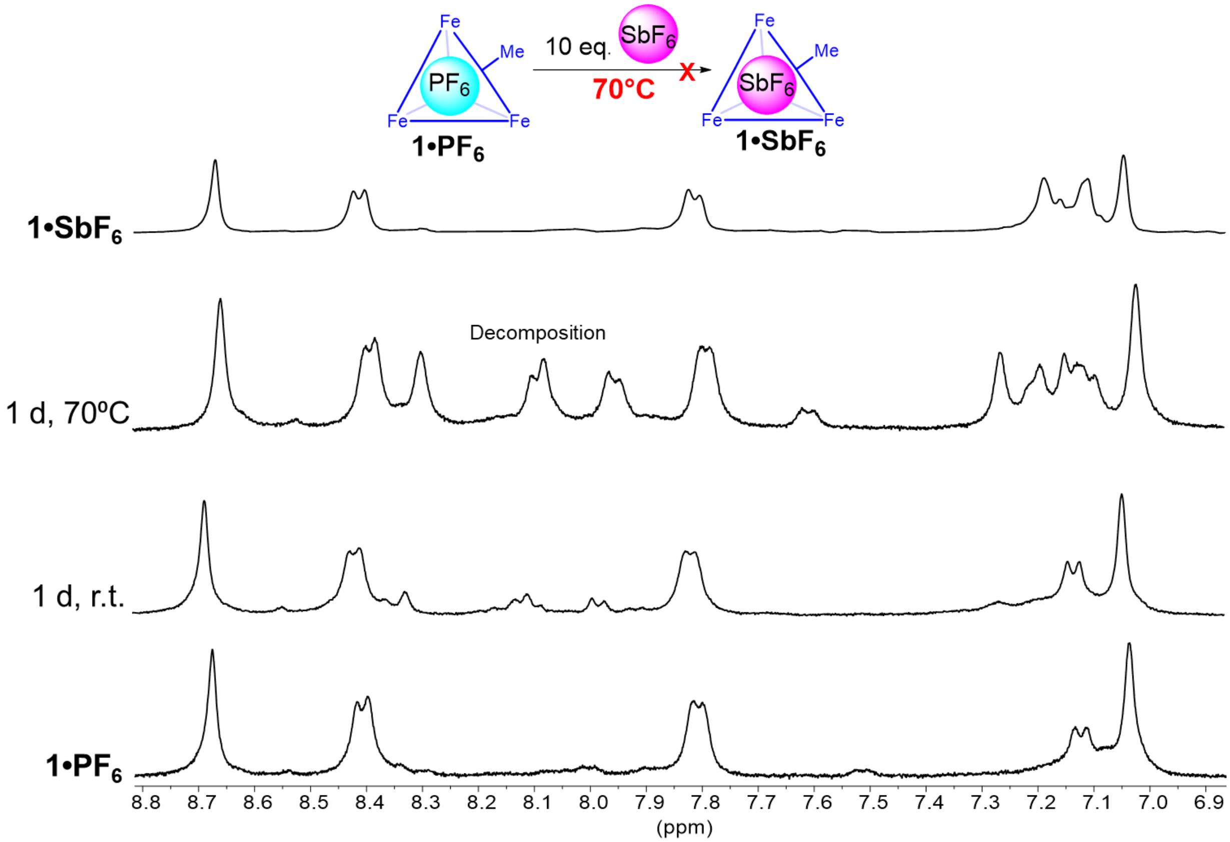

Figure S-56. [1]H NMR spectra of **1•PF₆** with 10 equivalents of $NaSbF_6$, over 1 day at 70ºC (D_2O, 400 MHz, 298K/343K). Related to Figure 7.

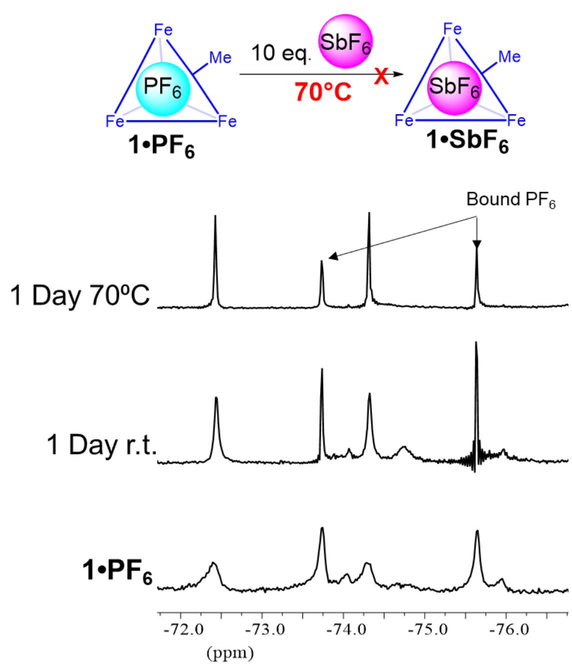

Figure S-57. [19]F NMR spectra of **1•PF₆** with 10 equivalents of $NaSbF_6$, over 1 day at 70ºC (D_2O, 376 MHz, 298K/343K). Related to Figure 7.

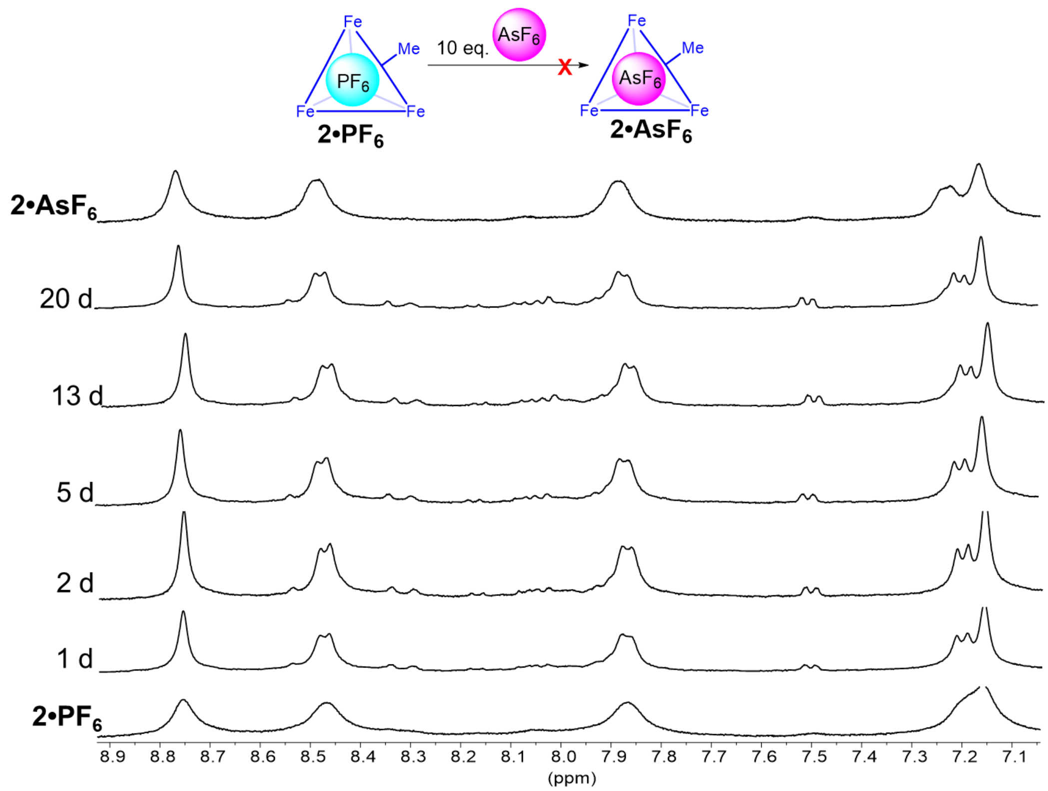

Figure S-58. ^{1}H NMR spectra of **2•PF₆** with 10 equivalents of $NaAsF_6$, over 14 days (D_2O, 400 MHz, 298K). Related to Figure 7.

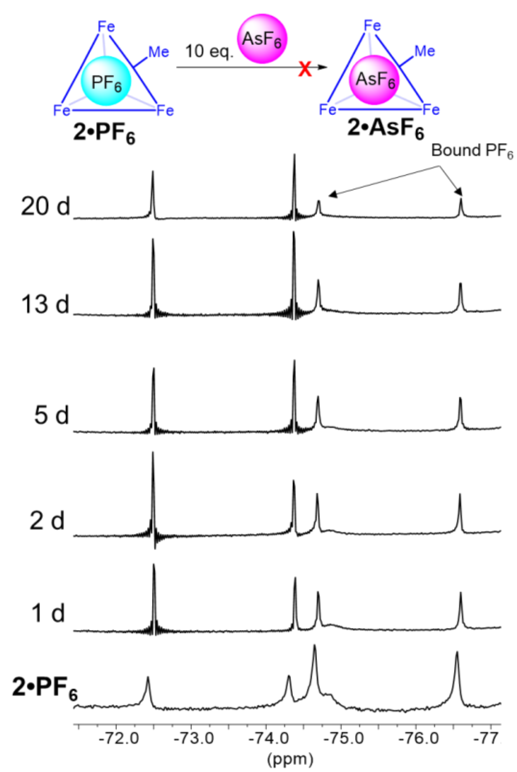

Figure S-59. ^{19}F NMR spectra of **2•PF₆** with 10 equivalents of $NaAsF_6$, over 14 days (D_2O, 376 MHz, 298K). Related to Figure 7.

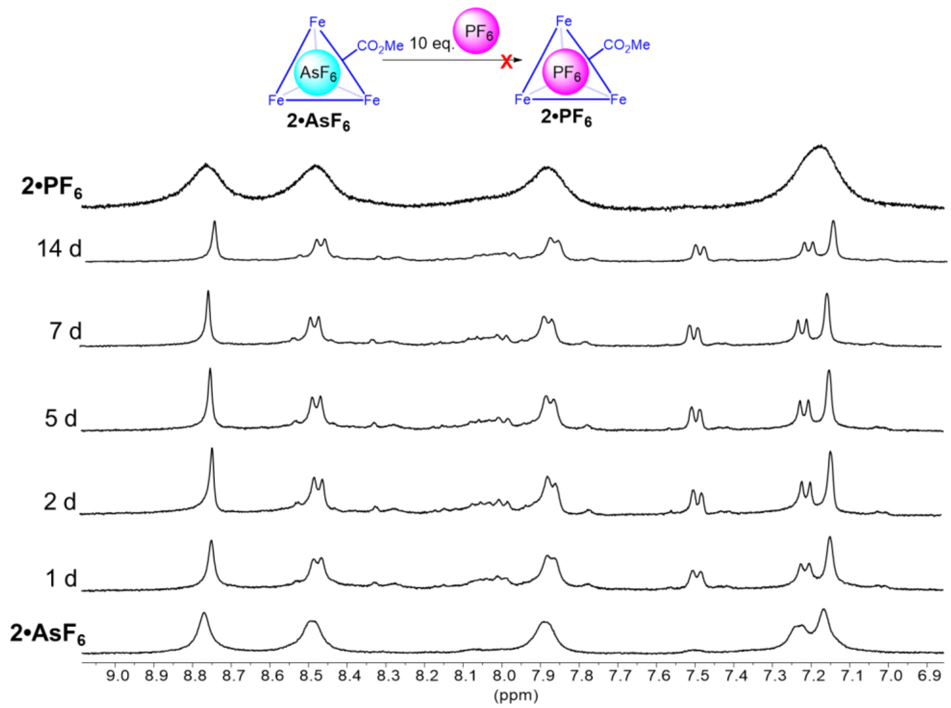

Figure S-60. [1]H NMR spectra of **2•AsF$_6$** with 10 equivalents of NaPF$_6$, over 14 days (D$_2$O, 400 MHz, 298K). Related to Figure 7.

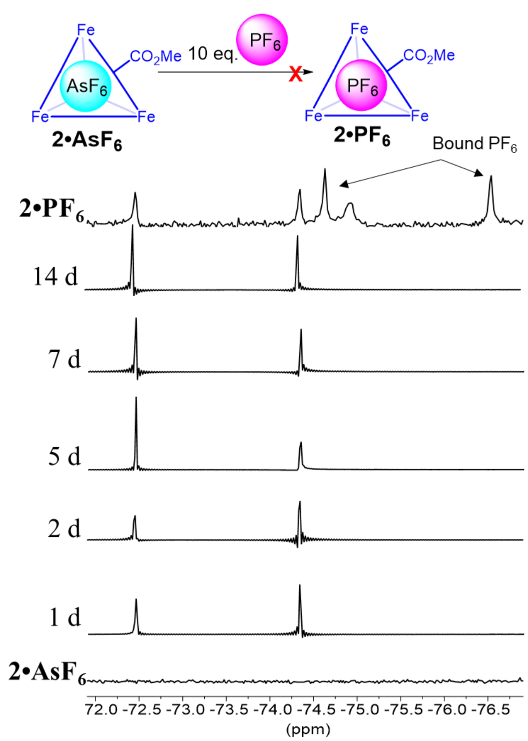

Figure S-61. [19]F NMR spectra of **2•AsF$_6$** with 10 equivalents of NaPF$_6$, over 14 days (D$_2$O, 376 MHz, 298K). Related to Figure 7.

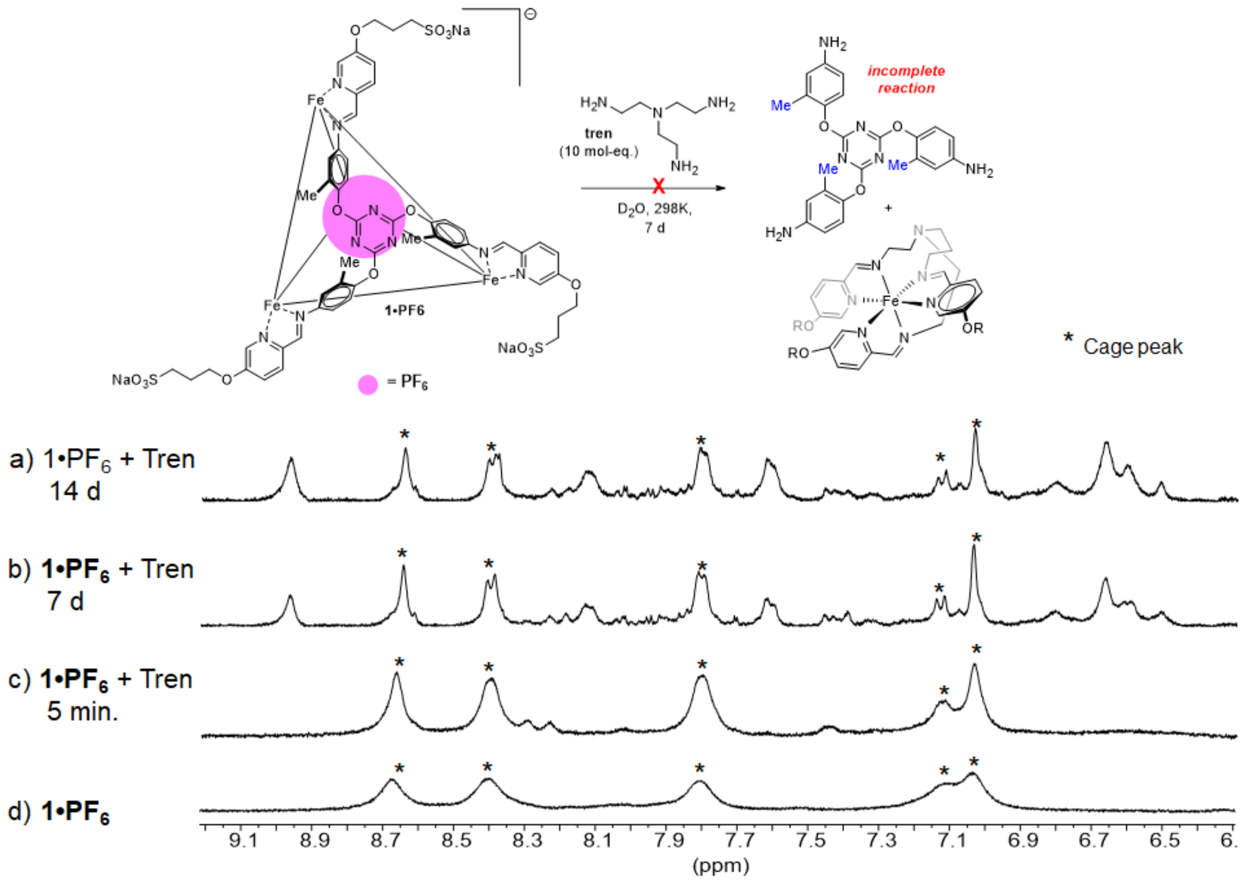

Figure S-62. [1]H NMR spectrum of d) **1•PF6**; and **1•PF6** with tris(2-aminoethyl)amine after c) 5 minutes; b) 1 week; and a) 2 weeks (D_2O, 400 MHz, 298K). Related to Figure 6.

Synthesis: Alternate Methods of Cage Assembly

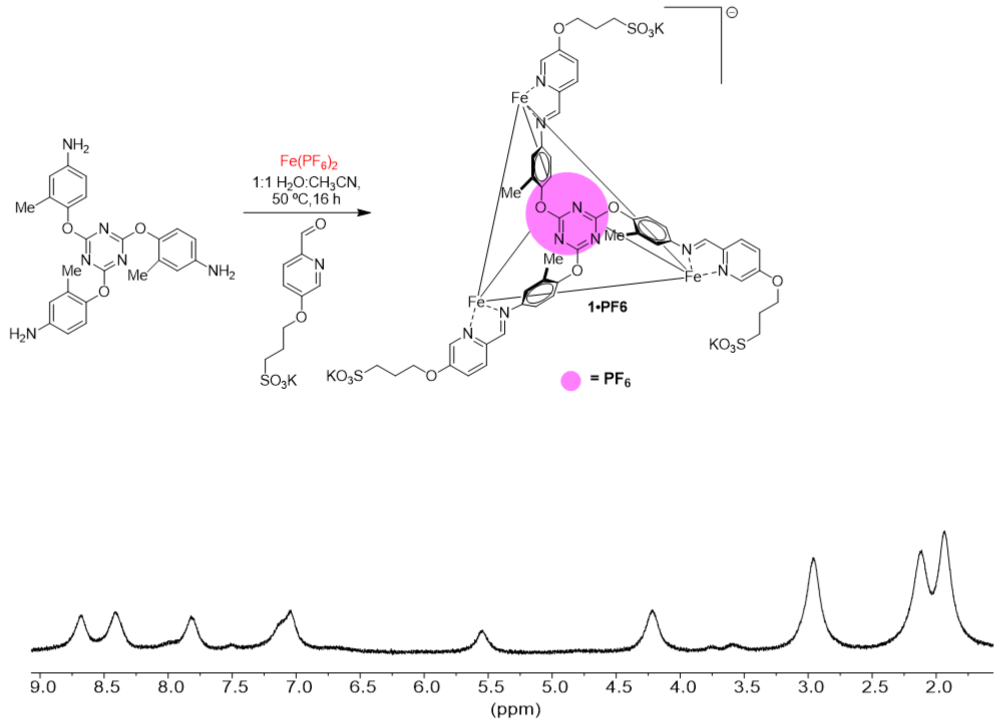

Figure S-63. ^{1}H NMR spectrum of cage **1•PF$_6$**, made with $Fe(PF_6)_2$ (D_2O, 400 MHz, 298K). Related to Figure 1.

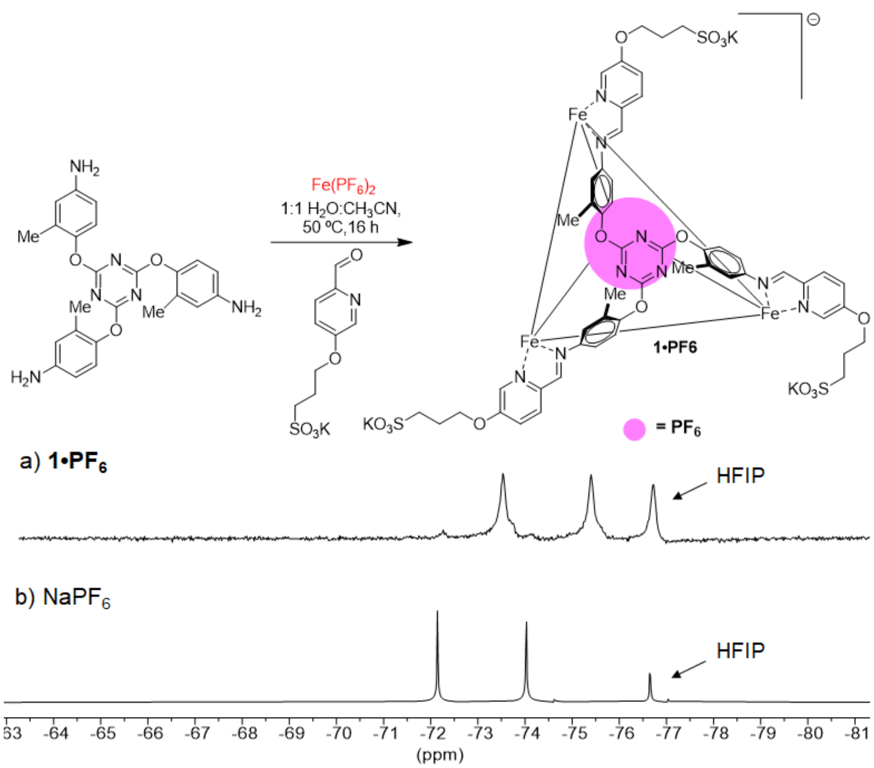

Figure S-64. ^{19}F NMR spectrum of a) **1•PF$_6$** made with $Fe(PF_6)_2$ and b) $NaPF_6$ with hexafluoroisopropanol (HFIP) as a standard (D_2O, 376 MHz, 298K). Related to Figure 1.

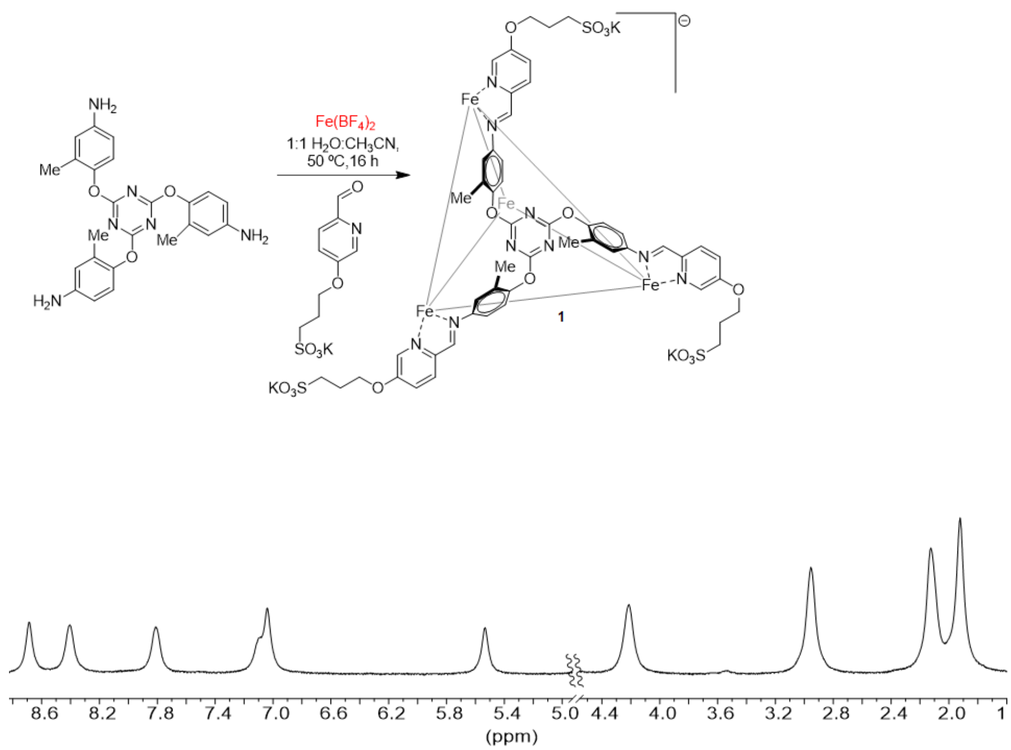

Figure S-65. ^{1}H NMR spectrum of cage **1**, made with $Fe(BF_4)_2$ (D_2O, 400 MHz, 298K). Related to Figure 1.

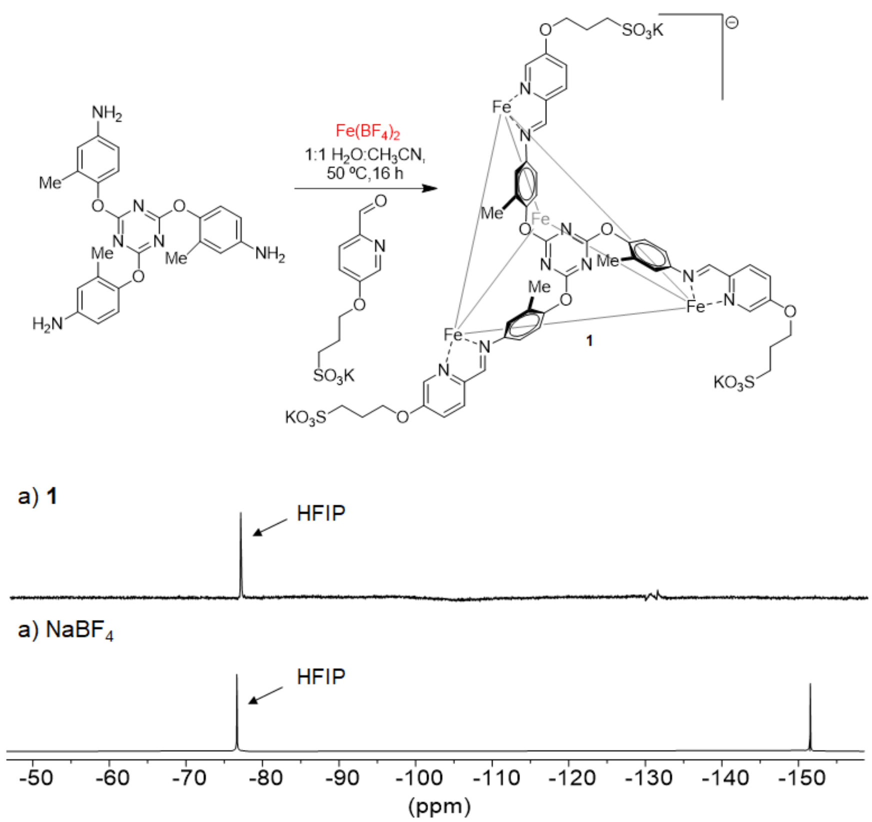

Figure S-66. ^{19}F NMR spectrum of a) **1** made with $Fe(BF_4)_2$ and b) $NaBF_4$ with hexafluoroisopropanol (HFIP) as a standard (D_2O, 376 MHz, 298K). Related to Figure 1.

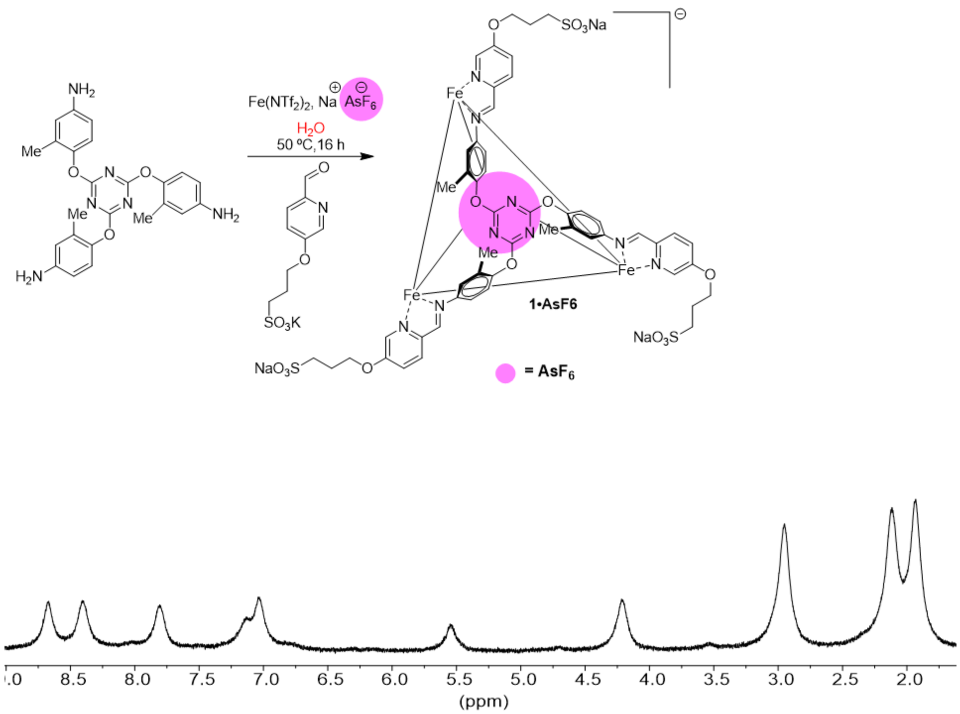

Figure S-67. ^{1}H NMR spectrum of cage **1•AsF$_6$**, made from pure water (D_2O, 400 MHz, 298K). Related to Figure 1.

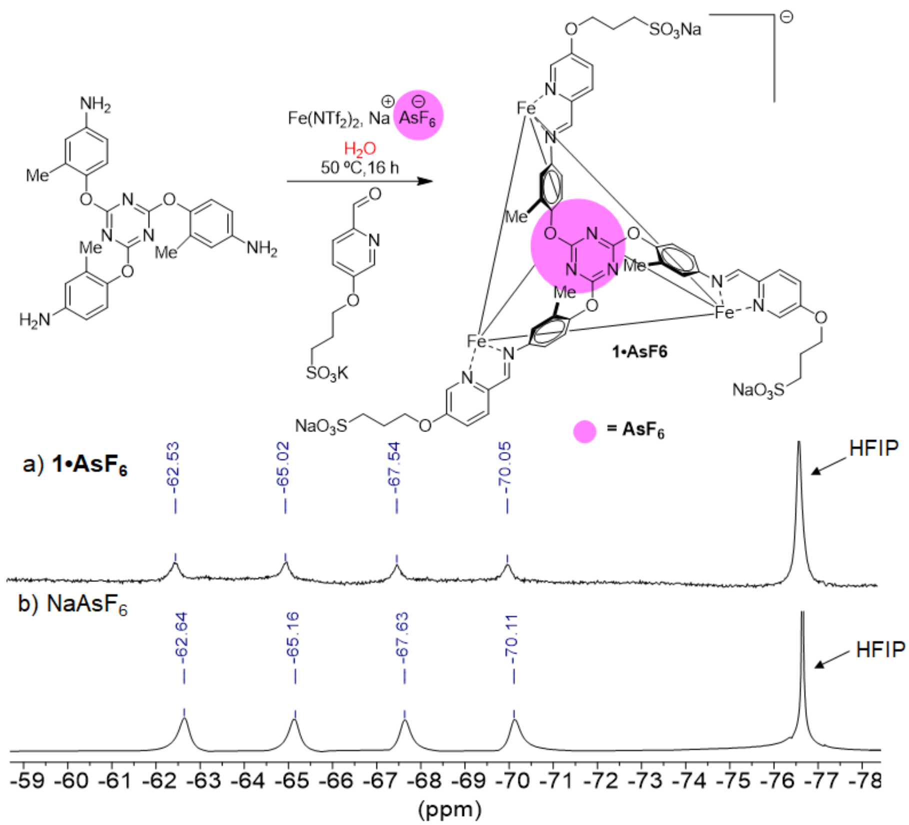

Figure S-68. ^{19}F NMR spectrum of a) **1•AsF$_6$**, made from pure water and b) $NaAsF_6$ with hexafluoroisopropanol (HFIP) as a standard (D_2O, 376 MHz, 298K). Related to Figure 1.

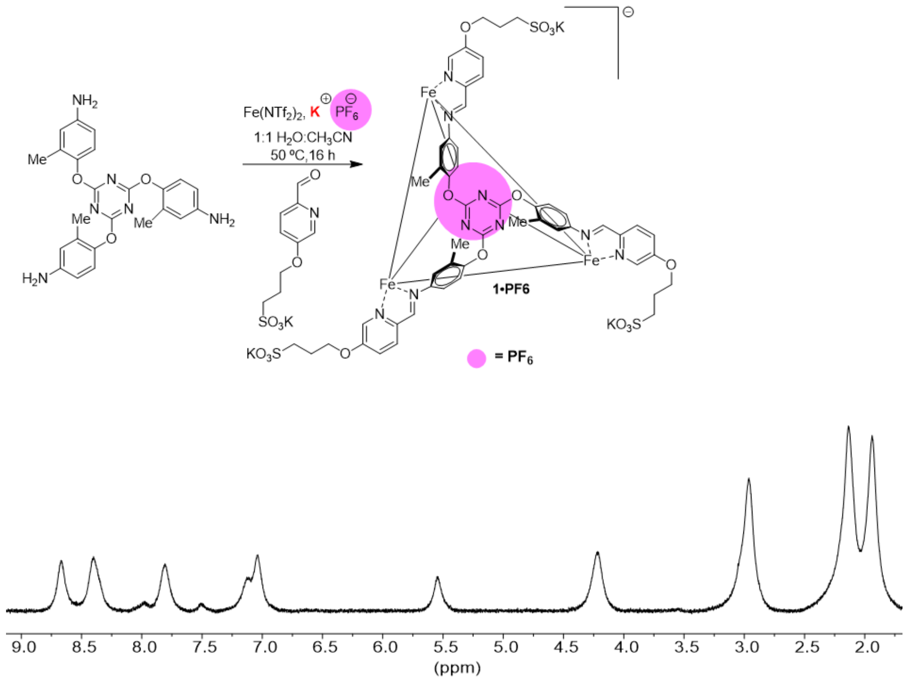

Figure S-69. [1]H NMR spectrum of cage **1•PF₆**, made with $Fe(NTf_2)_2$ and 10 equivalents of KPF_6 (D_2O, 400 MHz, 298K). Related to Figure 1.

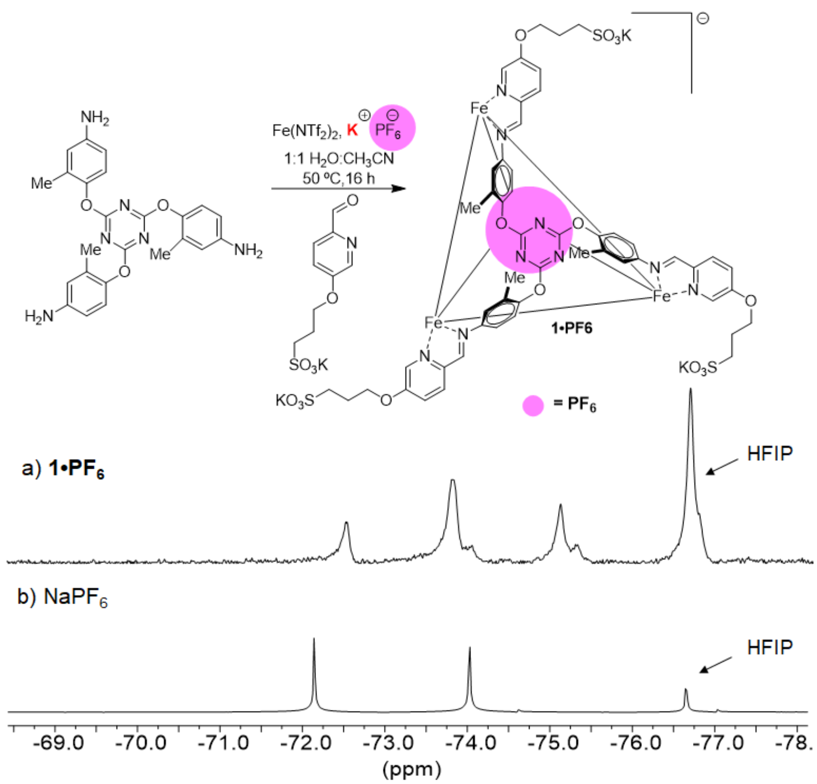

Figure S-70. [19]F NMR spectrum of a) **1•PF₆**, made from $Fe(NTf_2)_2$ and KPF_6 and b) $NaAsF_6$ with hexafluoroisopropanol (HFIP) as a standard (D_2O, 376 MHz, 298K). Related to Figure 1.

Characterization: ^{19}F NMR Spectra of Guests and Cages including HFIP Standards

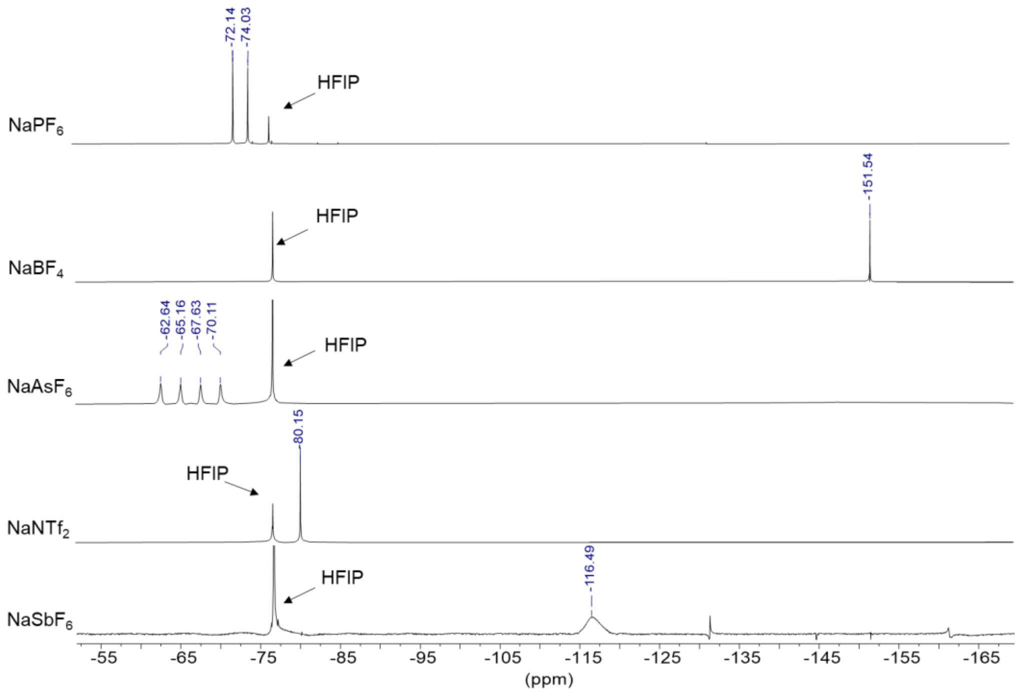

Figure S-71. ^{19}F NMR spectra of anionic guests with hexafluoroisopropanol (HFIP) as a standard (D_2O, 376 MHz, 298K). Related to Figure 3.

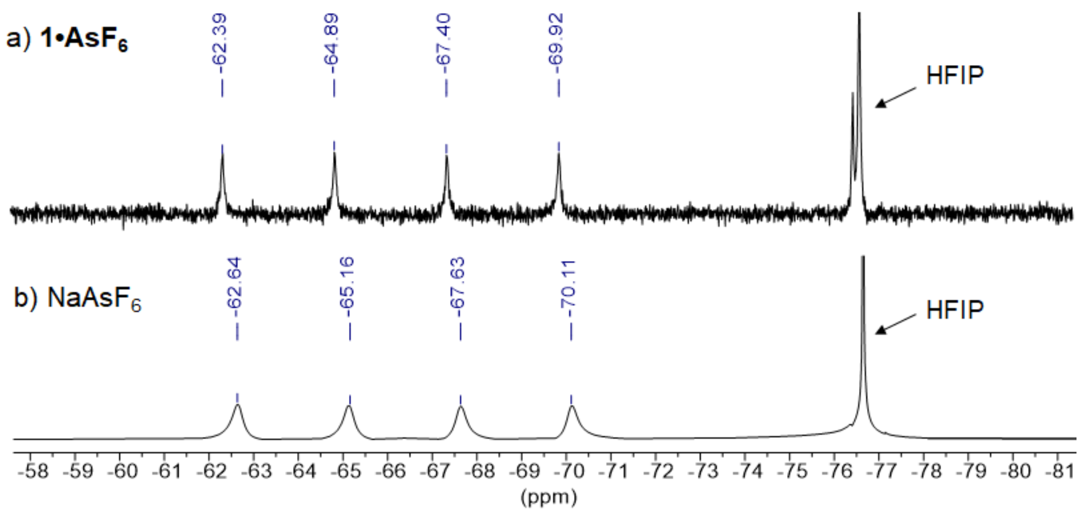

Figure S-72. ^{19}F NMR spectrum of a) **1•AsF$_6$** and b) $NaAsF_6$ with hexafluoroisopropanol (HFIP) as a standard (D_2O, 376 MHz, 298K). Related to Figure 3.

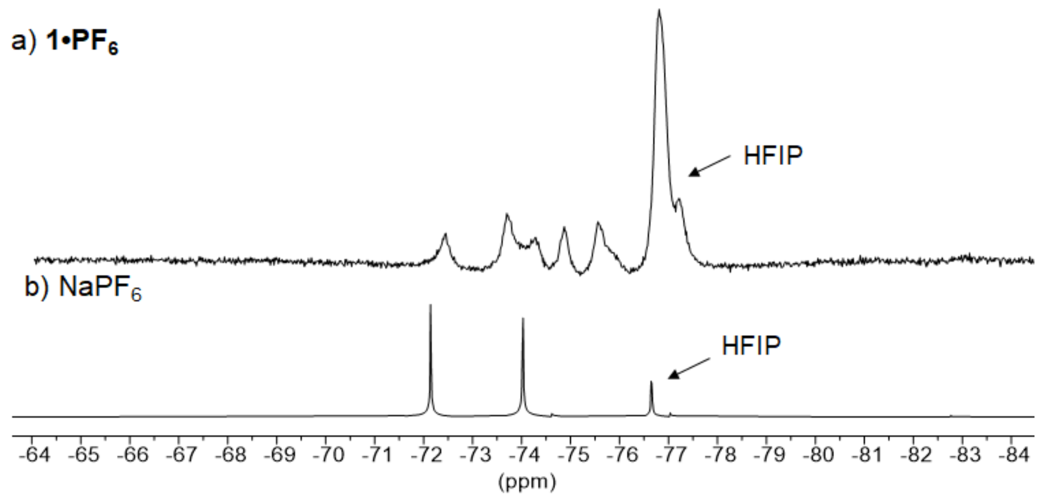

Figure S-73. ^{19}F NMR spectrum of a) **1•PF$_6$** and b) $NaPF_6$ with hexafluoroisopropanol (HFIP) as a standard (D_2O, 376 MHz, 298K). Related to Figure 3.

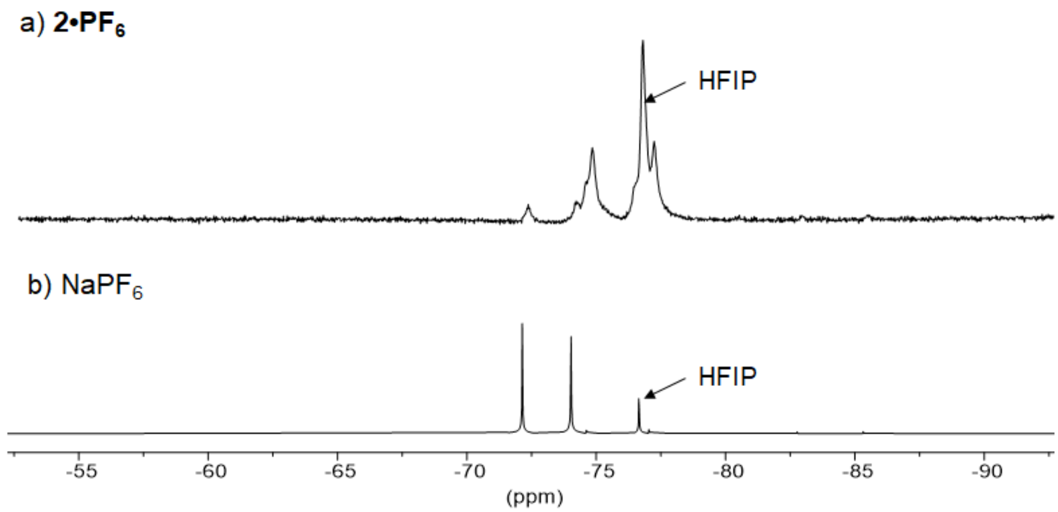

Figure S-74. ^{19}F NMR spectrum of a) **2•PF$_6$** and b) $NaPF_6$ with hexafluoroisopropanol (HFIP) as a standard (D_2O, 376 MHz, 298K). Related to Figure 3.